Appendix A. Supplementary material

Metal Dimers Embedded Vertically in Defect-graphene as Gas Sensors: A First-Principles Study

Linke Yu, Fengyu Li*

School of Physical Science and Technology, Inner Mongolia University, Hohhot, 010021, China

*Corresponding Author: fengyuli@imu.edu.cn (FL)

Table S1 The binding energy (E_b) per M atom of $M_2 \perp$ gra species, the cohesive energy (E_{coh}) of M metals (in eV).

structure	E_b	E_{coh}	structure	E_b	E_{coh}	structure	E_b	E_{coh}
2Sc-gra	**-5.90**	-4.34	2Y-gra	**-5.92**	-4.40			
2Ti-gra	**-5.93**	-5.51	2Zr-gra	**-6.64**	-6.45	2Hf-gra	**-7.07**	-6.71
2V-gra	**-4.96**	-5.34	2Nb-gra	-6.05	-7.04	2Ta-gra	-6.81	-8.37
2Cr-gra	-3.29	-4.07	2Mo-gra	-5.00	-6.33	2W-gra	-5.35	-8.41
2Mn-gra	**-4.28**	-3.79	2Tc-gra	-5.44	-6.88	2Re-gra	-4.99	-7.83
2Fe-gra	**-4.90**	-4.61	2Ru-gra	-6.44	-7.08	2Os-gra	-6.42	-8.51
2Co-gra	**-5.84**	-5.04	2Rh-gra	**-6.52**	-5.93	2Ir-gra	**-7.23**	-7.59
2Ni-gra	**-6.17**	-5.04	2Pd-gra	**-4.80**	-3.75	2Pt-gra	**-6.31**	-5.52
2Cu-gra	**-3.37**	-3.50	2Ag-gra	**-2.03**	-2.49	2Au-gra	-2.38	-2.99
2Zn-gra	**-0.98**	-1.11	2Cd-gra	**-0.57**	-0.75			

Table S2 The Bader charge (Q) on the M atoms, the band energy gap (E_g), the magnetic order (MO) and the magnetic moment on M atoms (M) of the five $M_2 \perp$ gra (M = Co, Ni, Rh, Ir and Pt) and M_1@gra (M = Co, Ni, Rh and Pt) structures.

system	Q ($\|e\|$)	E_g (eV)	MO	M (μ_B)
$Co_2 \perp$ gra	+0.67/+0.67	0.00	FM	0.66/0.66
$Ni_2 \perp$ gra	+0.68/+0.68	0.02	NM	0.00/0.00
$Rh_2 \perp$ gra	+0.35/+0.35	0.00	FM	0.24/0.24
$Ir_2 \perp$ gra	+0.39/+0.39	0.00	FM	0.24/0.24
$Pt_2 \perp$ gra	+0.30/+0.30	0.22	NM	0.00/0.00
Co_1@gra	+0.75	0.00		0.29
Ni_1@gra	+0.74	0.25	NM	0.00
Rh_1@gra	+0.43	0.00		0.17
Ir_1@gra	+0.82	0.00		0.26
Pt_1@gra	+0.50	0.18	NM	0.00

Table S3 The magnetic anisotropy energy (MAE, in meV/M atom) for the $M_2 \perp$ gra and M_2-gra with two M atoms on two sides and one side of graphene, respectively.

system	E(100)−E(001)	E(011)−E(001)	E(010)−E(001)	E(101)−E(001)	E(110)−E(001)	E(111)−E(001)
$Co_2 \perp$ gra	2.81	1.28	2.79	1.28	2.80	1.75
Co_2-gra	0.58	0.34	0.60	0.14	0.59	0.32
Rh_2-gra	5.39	2.72	5.38	2.52	5.37	3.50
Ir_2-gra	16.71	13.78	21.95	13.15	21.47	19.84
system	E(100)−E(010)	E(011)−E(010)	E(001)−E(010)	E(101)−E(010)	E(110)−E(010)	E(111)−E(010)
$Rh_2 \perp$ gra	0.01	0.11	0.20	0.11	0.01	0.08
$Ir_2 \perp$ gra	0.01	4.86	13.63	4.86	0.01	2.89

Table S4 The magnetic moment on M atoms of the three $M_2 \perp$ gra (M = Co, Rh and Ir) and three M_2−gra (M = Co, Rh and Ir) structures.

system	Co	Rh	Ir
$M_2 \perp$ gra	0.66/0.66	0.24/0.24	0.24/0.24
M_2−gra	0.03/1.91	0.04/1.33	0.08/1.50

Table S5 The binding energy (E_b) per M atom of $M_2 \perp$ gra, M_2-gra and M_1@gra species.

E_b	Co	Ni	Rh	Ir	Pt
$M_2 \perp$ gra	-5.84	-6.17	-6.52	-7.23	-6.31
M_2-gra	-5.13		-5.81	-7.12	
M_1@gra	-8.25	-7.52	-9.05	-10.28	-7.97

Table S6 The adsorption energy (E_{ad}), the charge transferred from the monolayer to molecule (ΔQ), the shortest distance between the molecule and monolayer (D), the band-gap widths (E_g), the recovery time (τ), the magnetic order (MO) and the magnetic moment on M atoms (M) for the structures of the molecules adsorbed on the $Co_2 \perp$ gra.

system	E_{ad} (eV)	ΔQ ($\|e\|$)	D (Å)	E_g (eV)	τ (s) 300 K	τ (s) 500 K	MO	M (μ_B)
O_2	-2.04	-0.69	1.86	0.00	3.72×10^{21}	1.41×10^{9}	FM	0.73/0.39
N_2	-1.49	-0.27	1.80	0.30	1.78×10^{12}	1.50×10^{3}	NM	
CO	-2.23	-0.27	1.79	0.30	6.16×10^{24}	1.63×10^{11}	NM	
CO_2	-1.02	-0.51	1.90	0.19	1.93×10^{4}	1.19×10^{-2}	NM	
NO	-3.05	-0.36	1.66	0.00	4.85×10^{38}	1.30×10^{20}	FM	0.02/0.27
NO_2	-2.87	-0.59	1.86	0.00	4.32×10^{35}	1.45×10^{18}	FM	0.05/0.06
NH_3	-1.66	+0.11	2.00	0.34	1.35×10^{15}	1.05×10^{5}	NM	
H_2O	-1.07	+0.05	1.98	0.31	1.35×10^{5}	4.12×10^{-2}	NM	
H_2S	-1.41	-0.00	2.17	0.29	7.83×10^{10}	2.04×10^{2}	NM	
SO_2	-1.57	-2.34	2.06	0.26	4.03×10^{13}	1.11×10^{4}	NM	

Table S7 The adsorption energy (E_{ad}), the charge transferred from the monolayer to molecule (ΔQ), the shortest distance between the molecule and monolayer (D), the band-gap widths (E_g), the recovery time (τ), the magnetic order (MO) and the magnetic moment on M atoms (M) for the structures of the molecules adsorbed on the $Ni_2 \perp$ gra.

system	E_{ad} (eV)	ΔQ ($\|e\|$)	D (Å)	E_g (eV)	τ (s) 300 K	τ (s) 500 K	MO	M (μ_B)
O_2	-1.30	-0.62	1.93	0.00	1.07×10^{9}	13.0	FM	+0.14/+0.06
N_2	-0.73	-0.27	1.85	0.09	2.35×10^{-1}	8.43×10^{-6}	NM	
CO	-1.46	-0.27	1.81	0.10	5.51×10^{11}	7.11×10^{2}	NM	
CO_2	-0.22	-0.51	2.02	0.01	5.35×10^{-10}	2.45×10^{-11}	NM	
NO	-2.08	-0.40	1.74	0.08	1.77×10^{22}	3.83×10^{9}	AFM	-0.05/+0.13
NO_2	-2.09	-0.58	1.94	0.00	2.61×10^{22}	4.92×10^{9}	FM	+0.21/+0.14
NH_3	-1.20	+0.11	2.05	0.02	2.16×10^{7}	1.07	NM	
H_2O	-0.68	+0.05	2.04	0.00	3.31×10^{-2}	2.40×10^{-6}	NM	
H_2S	-0.94	+0.00	2.25	0.03	8.50×10^{2}	1.61×10^{-3}	NM	
SO_2	-1.03	-2.34	2.20	0.06	2.85×10^{4}	1.52×10^{-2}	NM	

Table S8 The adsorption energy (E_{ad}), the charge transferred from the monolayer to molecule (ΔQ), the shortest distance between the molecule and monolayer (D), the band-gap widths (E_g), the recovery time (τ), the magnetic order (MO) and the magnetic moment on M atoms (M) for the structures of the molecules adsorbed on the $Rh_2 \perp$ gra.

system	E_{ad} (eV)	ΔQ ($\|e\|$)	D (Å)	E_g (eV)	τ (s) 300 K	MO	M (μ_B)
O_2	-1.48	-0.47	1.95	0.00	1.20×10^{12}	FM	+0.01/+0.01
N_2	-0.92	-0.19	2.00	0.23	3.89×10^{2}	NM	
CO	-1.78	-0.19	1.79	0.24	1.46×10^{17}	NM	
CO_2	-0.38	-0.39	2.02	0.00	2.75×10^{-7}	NM	
NO	-2.65	-0.29	1.74	0.00	8.08×10^{31}	NM	
NO_2	-2.57	-0.50	1.94	0.00	3.56×10^{30}	NM	
NH_3	-1.30	+0.16	2.05	0.24	1.07×10^{9}	NM	
H_2O	-0.70	+0.06	2.04	0.23	7.23×10^{-2}	NM	
H_2S	-1.13	+0.10	2.25	0.23	1.41×10^{6}	NM	
SO_2	-1.23	-2.29	2.20	0.18	6.98×10^{7}	NM	

Table S9 The adsorption energy (E_{ad}), the charge transferred from the monolayer to molecule (ΔQ), the shortest distance between the molecule and monolayer (D), the band-gap widths (E_g), the recovery time (τ), the magnetic order (MO) and the magnetic moment on M atoms (M) for the structures of the molecules adsorbed on the $Ir_2 \perp$ gra.

system	E_{ad} (eV)	ΔQ ($\|e\|$)	D (Å)	E_g (eV)	τ (s) 300 K	MO	M (μ_B)
O_2	-1.88	-0.82	1.91	0.00	7.22×10^{18}	FM	+0.15/+0.37
N_2	-1.33	-0.36	1.91	0.00	3.45×10^{9}	FM	+0.07/+0.32
CO	-2.78	-0.39	1.84	0.16	1.29×10^{34}	NM	
CO_2	-0.63	-0.52	2.07	0.00	4.74×10^{-3}	NM	
NO	-3.19	-0.47	1.81	0.00	1.14×10^{41}	NM	
NO_2	-2.87	-0.60	2.00	0.00	4.32×10^{35}	NM	
NH_3	-1.47	+0.15	2.17	0.00	8.14×10^{11}	FM	+0.22/+0.52
H_2O	-0.76	+0.07	2.20	0.00	7.51×10^{-1}	FM	+0.28/+0.54
H_2S	-1.43	+0.06	2.28	0.00	1.71×10^{11}	FM	+0.15/+0.48
SO_2	-1.50	-2.30	2.20	0.00	2.63×10^{12}	FM	+0.16/+0.43

Table S10 The adsorption energy (E_{ad}), the charge transferred from the monolayer to molecule (ΔQ), the shortest distance between the molecule and monolayer (D), the band-gap widths (E_g), the recovery time (τ), the magnetic order (MO) and the magnetic moment on M atoms (M) for the structures of the molecules adsorbed on the $Pt_2 \perp$ gra.

system	E_{ad} (eV)	ΔQ ($\|e\|$)	D (Å)	E_g (eV)	τ (s) 300 K	MO	M (μ_B)
O_2	-0.91	-0.54	2.17	0.00	2.64×10^{2}	FM	+0.04/+0.03
N_2	-0.53	-0.17	2.02	0.07	9.58×10^{-5}	NM	
CO	-1.62	-0.20	1.91	0.04	2.84×10^{14}	NM	
CO_2	-0.06	-0.25	2.20	0.00	1.04×10^{-12}	NM	
NO	-1.91	-0.37	1.85	0.06	2.33×10^{19}	AFM	-0.03/+0.09
NO_2	-1.88	-0.58	2.14	0.00	7.22×10^{18}	FM	+0.02/+0.03
NH_3	-1.15	+0.17	2.24	0.21	3.08×10^{6}	NM	
H_2O	-0.54	+0.07	2.40	0.22	1.40×10^{-4}	NM	
H_2S	-0.60	+0.05	2.33	0.16	1.47×10^{-3}	NM	
SO_2	-0.97	-2.26	2.29	0.01	2.74×10^{3}	NM	

Table S11 The adsorption energy (E_{ad}), the shortest distance between the molecule and monolayer (D), the band-gap widths (E_g) and the magnetic moment on M atoms (M) for the structures of the O_2/CO_2 (gas) and O_2+H_2O/CO_2+H_2O (mol+H_2O) adsorbed on the $Ni_2 \perp$ gra/$Pt_2 \perp$ gra.

system	E_{ad} (eV)		D (Å)		E_g (eV)		M (μ_B)	
system	gas	gas+H_2O	gas	gas+H_2O	gas	gas+H_2O	gas	gas+H_2O
Ni (O_2)	-1.30	-1.30	1.93	1.97	0.00	0.00	+0.14/+0.06	+0.10/+0.02
Pt (CO_2)	-0.06	-0.04	2.20	2.43	0.00	0.16	0.00/0.00	0.00/0.00

Table S12 The adsorption energy (E_{ad}) and the recovery time (τ) for the structures of the O_2 adsorbed on the $Ni_2 \perp$ gra and the CO_2 adsorbed on the $Pt_2 \perp$ gra.

system	E_{ad} (eV)		D (Å)		τ (s) 300K	
	DFT	DFT+U	DFT	DFT+U	DFT	DFT+U
Ni (O_2)	-1.30	-1.16	1.93	1.93	1.07×10^{9}	4.54×10^{9}
Pt (CO_2)	-0.06	-0.04	2.20	2.24	1.04×10^{-12}	4.76×10^{-13}

Table S13 The adsorption energy (E_{ad}), the shortest distance between the molecule and monolayer (D), the charge on the metal atom M (Q) and the magnetic moment on M atoms (M) for the structures of the molecules adsorbed on the $Rh_2\perp$gra and Rh_1@gra.

	E_{ad} (eV)		D (Å)		Q ($\|e\|$)		M (μ_B)	
system	Rh_2	Rh_1	Rh_2	Rh_1	Rh_2	Rh_1	Rh_2	Rh_1
O_2	-1.48	-1.30	1.95	2.13	+0.63/+0.37	+0.80	0.01/0.01	0.05
N_2	-0.92	-0.37	2.00	2.20	+0.49/+0.42	+0.57	0	0.09
CO	-1.78	-0.99	1.79	2.04	+0.43/+0.40	+0.57	0	0.05
CO_2	-0.38	-0.13	2.02	2.20	+0.47/+0.35	+0.56	0	0
NO	-2.65	-1.77	1.74	1.98	+0.58/+0.37	+0.67	0	0
NO_2	-2.57	-2.30	1.94	2.13	+0.61/+0.38	+0.69	0	0
NH_3	-1.30	-0.80	2.05	2.32	+0.42/+0.35	+0.52	0	0.18
H_2O	-0.70	-0.42	2.04	2.37	+0.46/+0.35	+0.56	0	0.20
H_2S	-1.13	-0.59	2.25	2.46	+0.34/+0.36	+0.47	0	0.16
SO_2	-1.23	-0.86	2.20	2.55	+0.37/+0.39	+0.54	0	0.02

Table S14 The d-band centers ($C_{d\text{-}band}$, in eV) of $M_2\perp$gra and M_1@gra

system	$C_{d\text{-}band}$	system	$C_{d\text{-}band}$
$Co_2\perp$gra	-0.93	Co_1@gra	-1.78
$Ni_2\perp$gra	-2.09	Ni_1@gra	-3.25
$Rh_2\perp$gra	-1.33	Rh_1@gra	-2.48
$Ir_2\perp$gra	-1.27	Ir_1@gra	-2.94
$Pt_2\perp$gra	-3.20	Pt_1@gra	-4.20

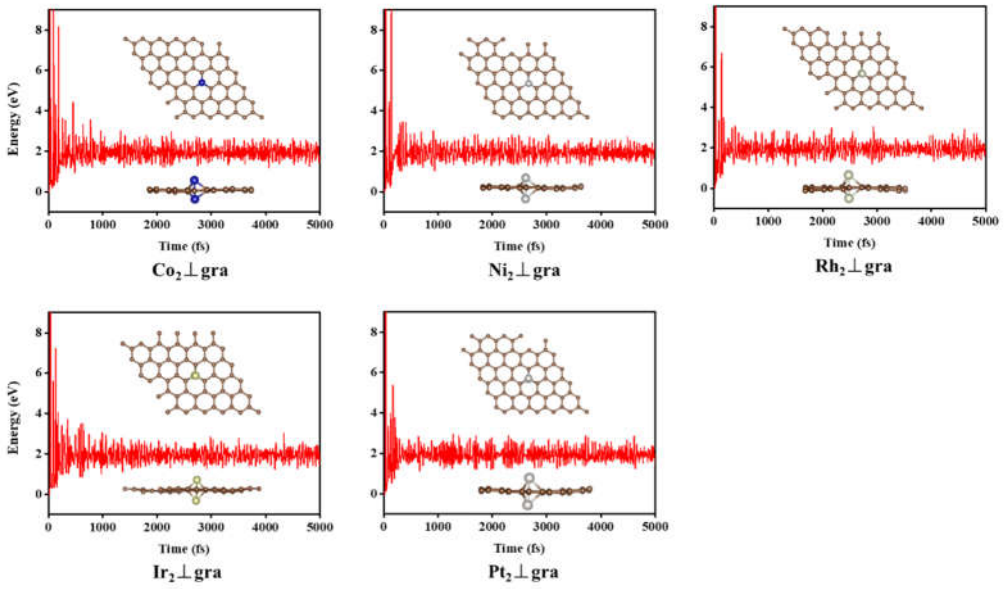

Fig. S1 The energy evolution of five $M_2\perp$gra (M = Co, Ni, Rh, Ir and Pt) monolayers during 5 ps FPMD simulation at 300 K, the insets are the final annealed structures.

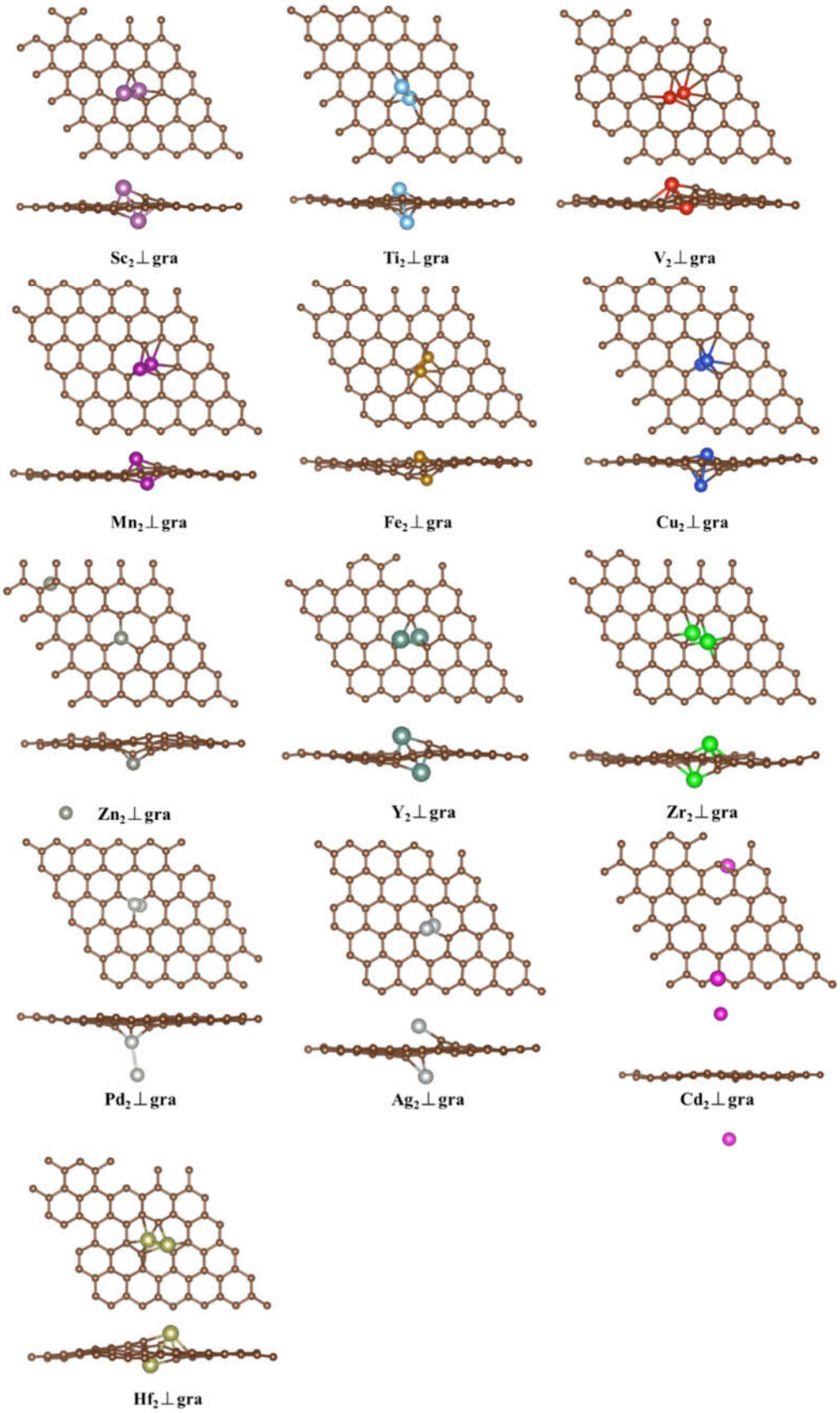

Fig. S2 The final structures of thirteen $M_2 \perp$ gra (M = Sc, Ti, V, Mn, Fe, Cu, Zn, Y, Zr, Pd, Ag, Cd and Hf) monolayers annealed for 5 ps at 300 K.

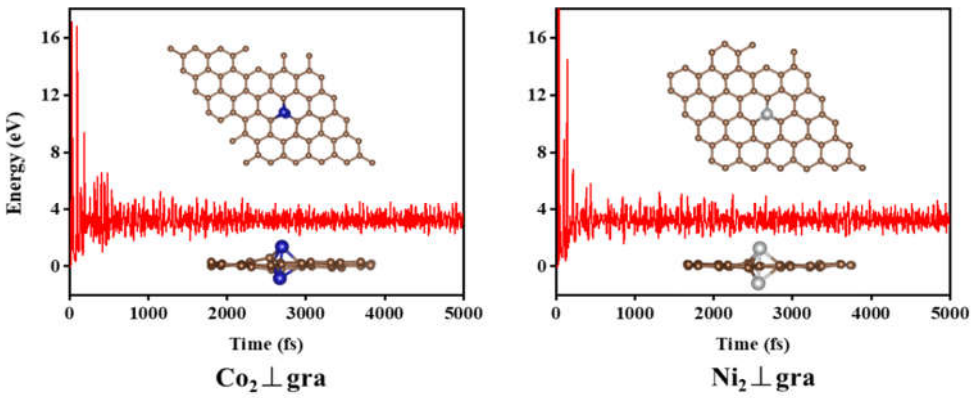

Fig. S3 The energy evolution of $Co_2 \perp$ gra (left) and $Ni_2 \perp$ gra (right) monolayers during 5 ps FPMD simulation at 500 K, the insets are the final annealed structures.

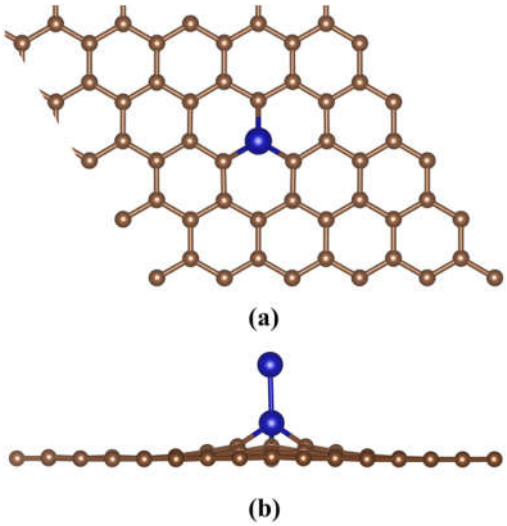

Fig. S4 Structural diagram of the M_2-gra model, top view (a) and side view (b). Color scheme: C, brown; M, blue.

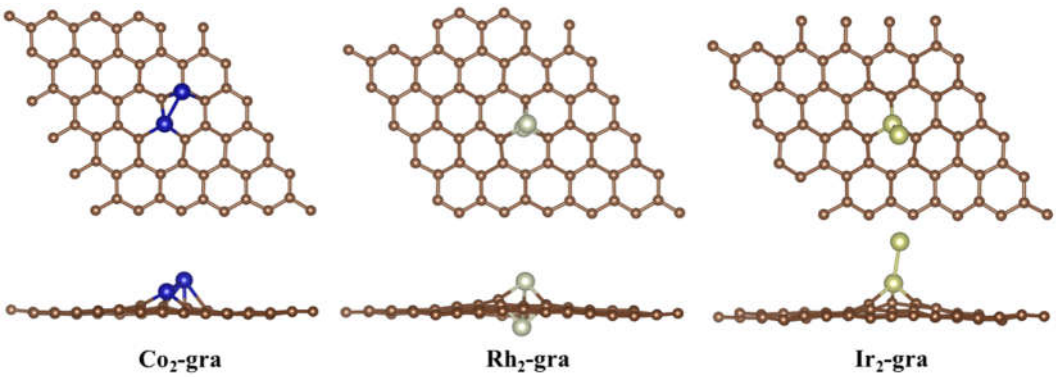

Fig. S5 The final structures of Co_2-gra, Rh_2-gra and Ir_2-gra monolayers annealed for 5 ps at 300 K.

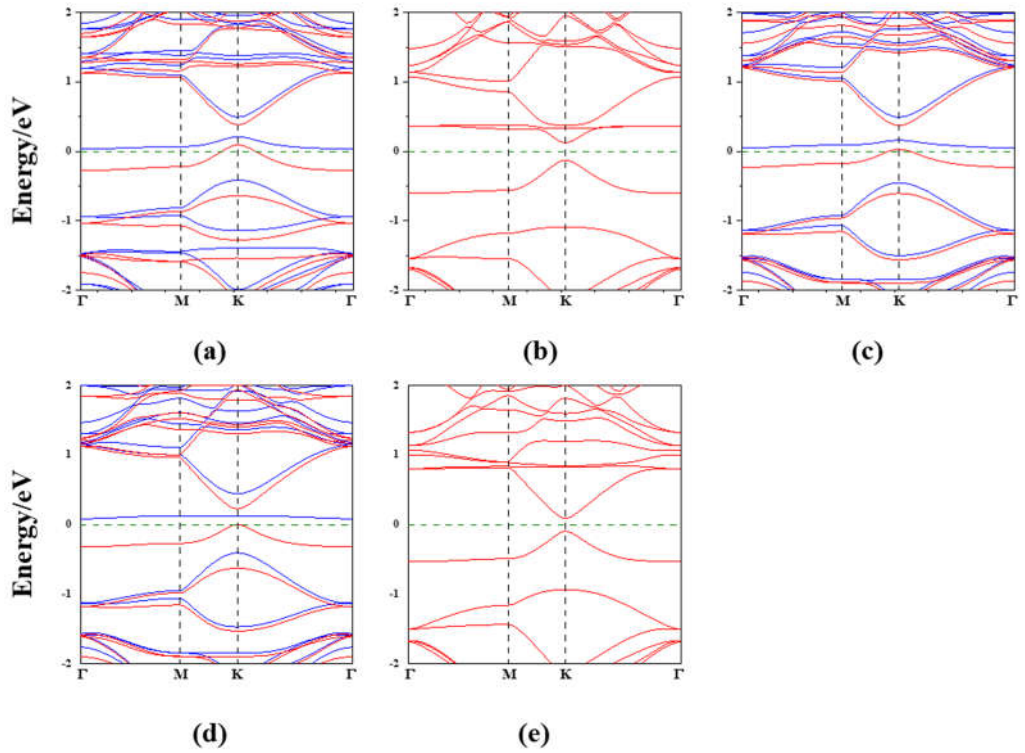

Fig. S6 The band structures of the five M_1@gra structures: Co_1@gra (a), Ni_1@gra (b), Rh_1@gra (c), Ir_1@gra (d) and Pt_1@gra (e).

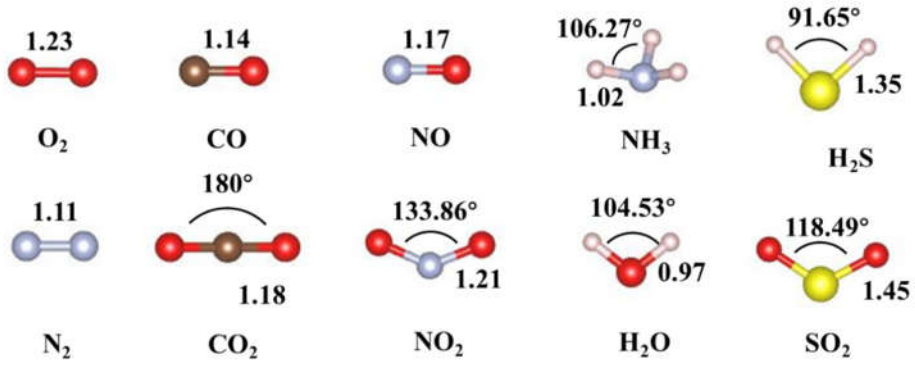

Fig. S7 The optimized structures of free gas molecules.

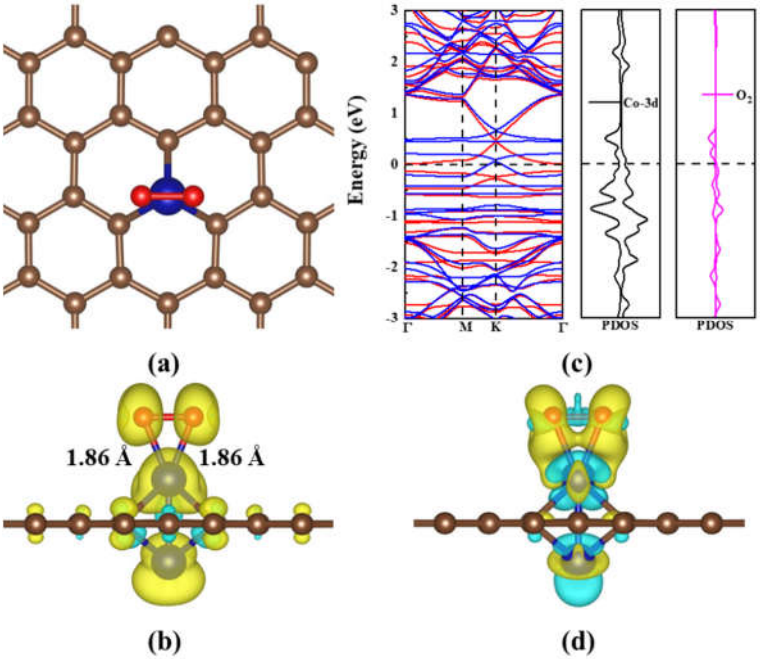

Fig. S8 The most favorable configuration of O_2 adsorption energy on the Co_2⊥gra structure (top view (a)), spatial spin density distribution (b), energy band structure and PDOS (c), and CDD diagram (d) of the adsorbed system. The isosurface value was set 0.003 e/Å^{-3}.

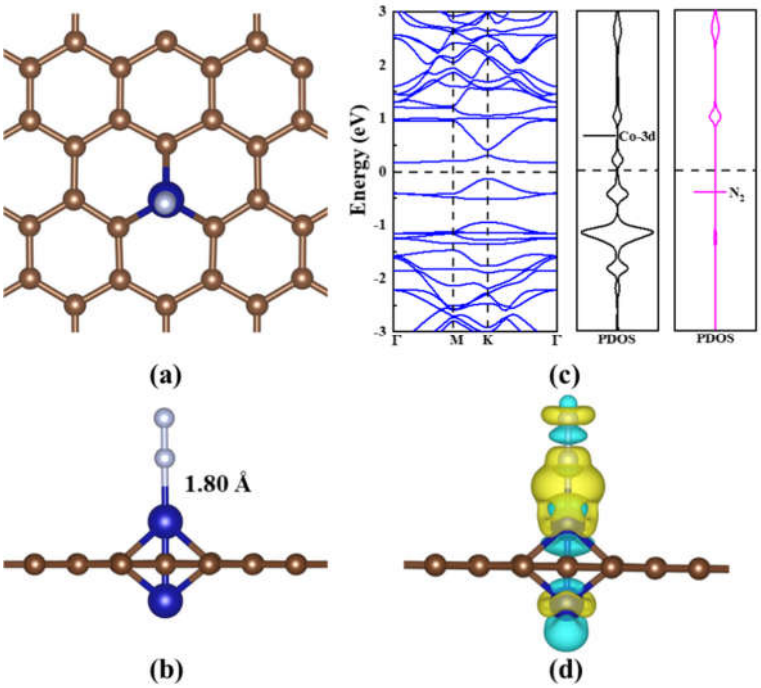

Fig. S9 The most favorable configuration of N_2 adsorption energy on the Co_2⊥gra structure (top view (a) and side view (b)), energy band structure and PDOS (c), and CDD diagram (d). The isosurface value was set 0.003 e/Å^{-3}.

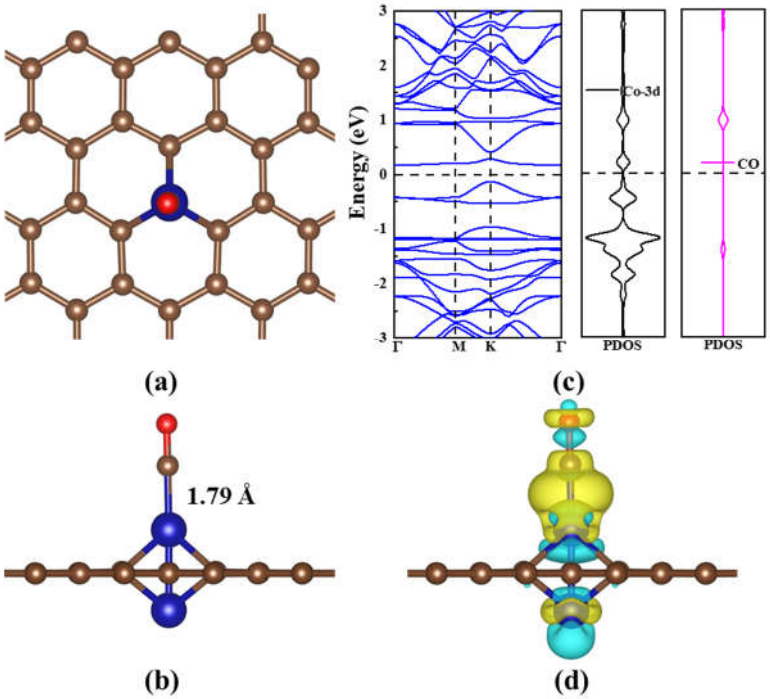

Fig. S10 The most favorable configuration of CO adsorption energy on the $Co_2 \perp$ gra structure (top view (a) and side view (b)), energy band structure and PDOS (c), and CDD diagram (d). The isosurface value was set 0.003 e/Å^{-3}.

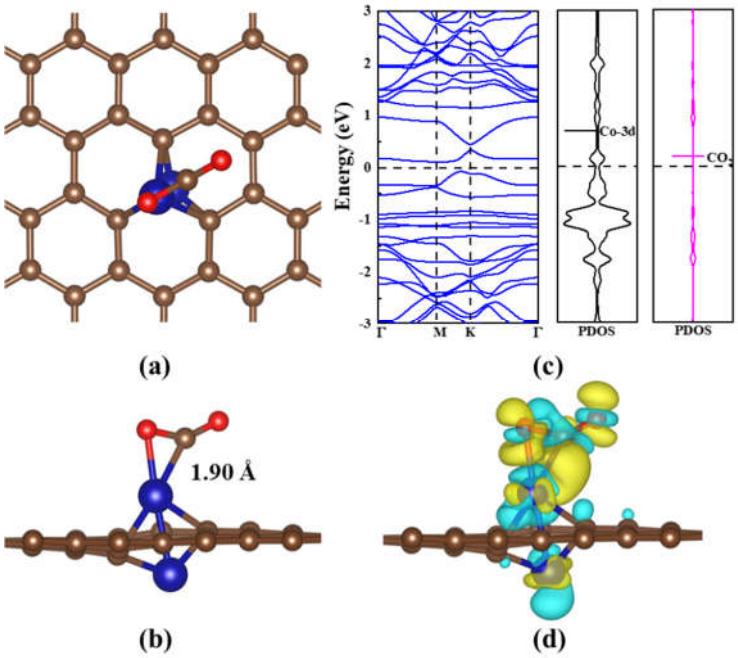

Fig. S11 The most favorable configuration of CO_2 adsorption energy on the $Co_2 \perp$ gra structure (top view (a) and side view (b)), energy band structure and PDOS (c), and CDD diagram (d). The isosurface value was set 0.003 e/Å^{-3}.

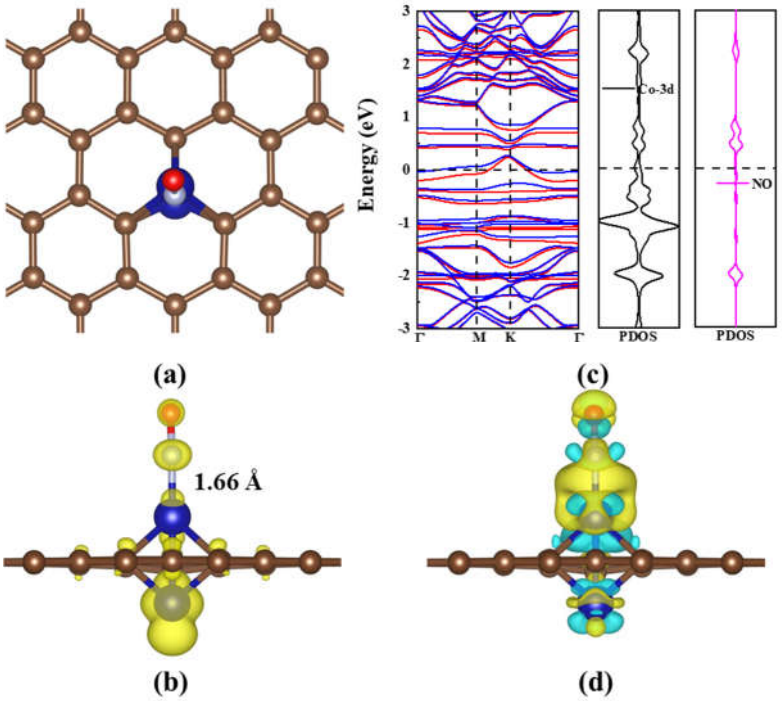

Fig. S12 The most favorable configuration of NO adsorption energy on the Co_2⊥gra structure (top view (a)), spatial spin density distributions (b), energy band structure and PDOS (c), and CDD diagram (d). The isosurface value was set 0.003 e/Å^{-3}.

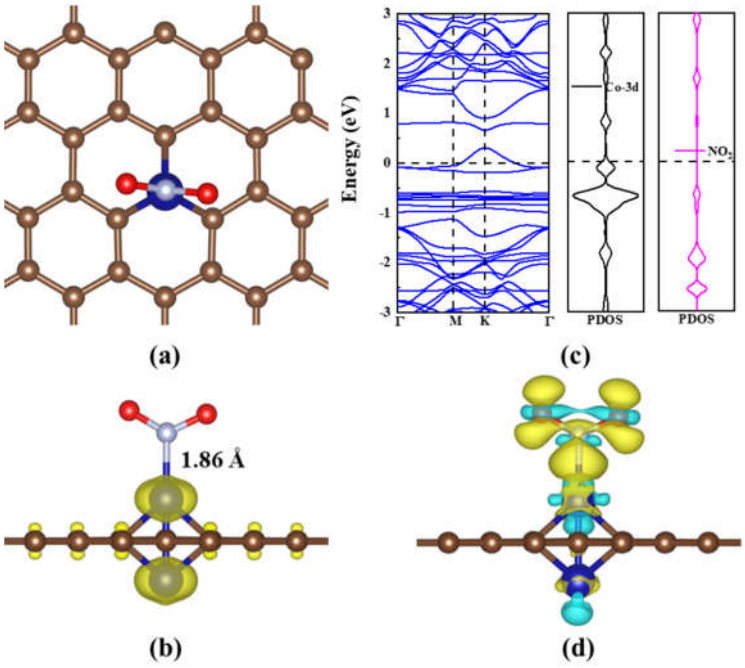

Fig. S13 The most favorable configuration of NO_2 adsorption energy on the Co_2⊥gra structure (top view (a)), spatial spin density distributions (b), energy band structure and PDOS (c), and CDD diagram (d). The isosurface value was set 0.0008 e/Å^{-3} for spatial spin density distributions and 0.003 e/Å^{-3} for CDD, respectively.

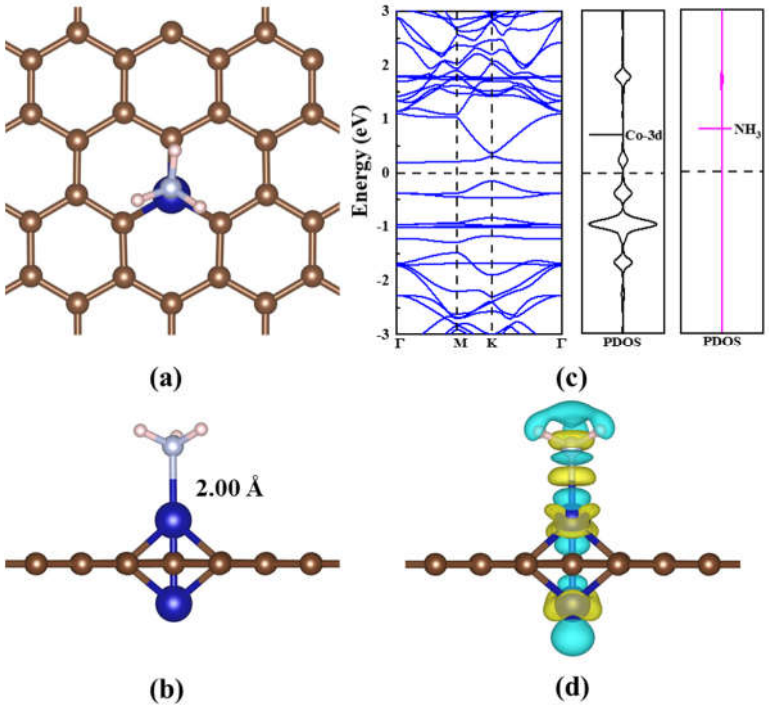

Fig. S14 The most favorable configuration of NH_3 adsorption energy on the Co_2⊥gra structure (top view (a) and side view (b)), energy band structure and PDOS (c), and CDD diagram (d). The isosurface value was set 0.003 e/Å^{-3}.

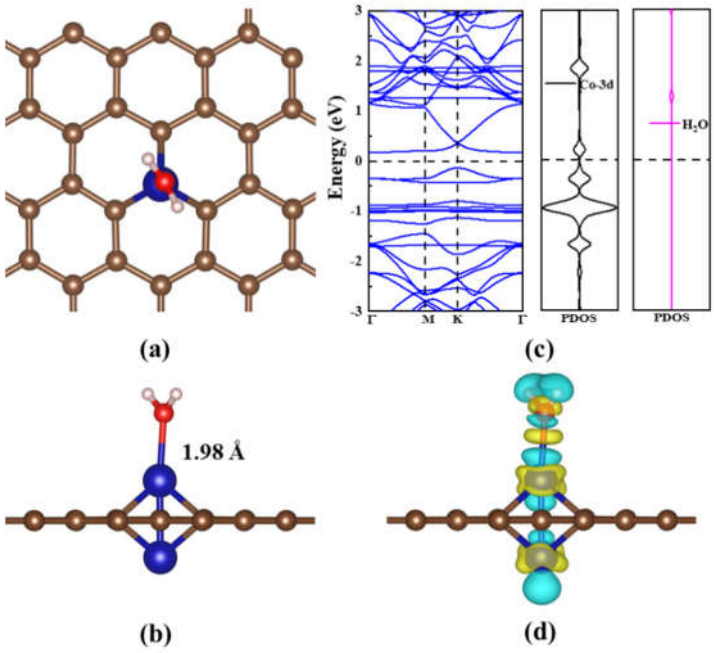

Fig. S15 The most favorable configuration of H_2O adsorption energy on the Co_2⊥gra structure (top view (a) and side view (b)), energy band structure and PDOS (c), and CDD diagram (d). The isosurface value was set 0.003 e/Å^{-3}.

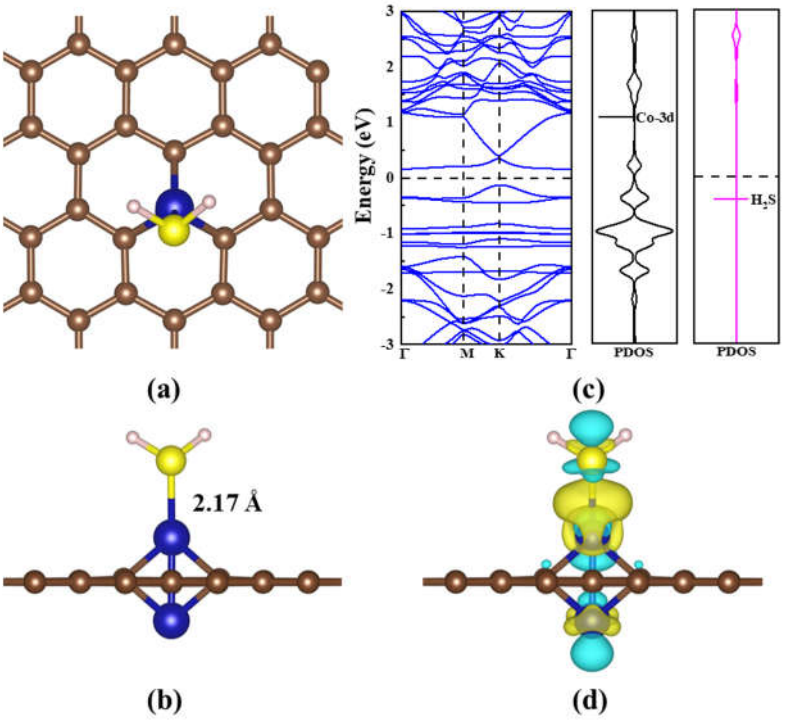

Fig. S16 The most favorable configuration of H_2S adsorption energy on the Co_2⊥gra structure (top view (a) and side view (b)), energy band structure and PDOS (c), and CDD diagram (d). The isosurface value was set 0.003 e/Å^{-3}.

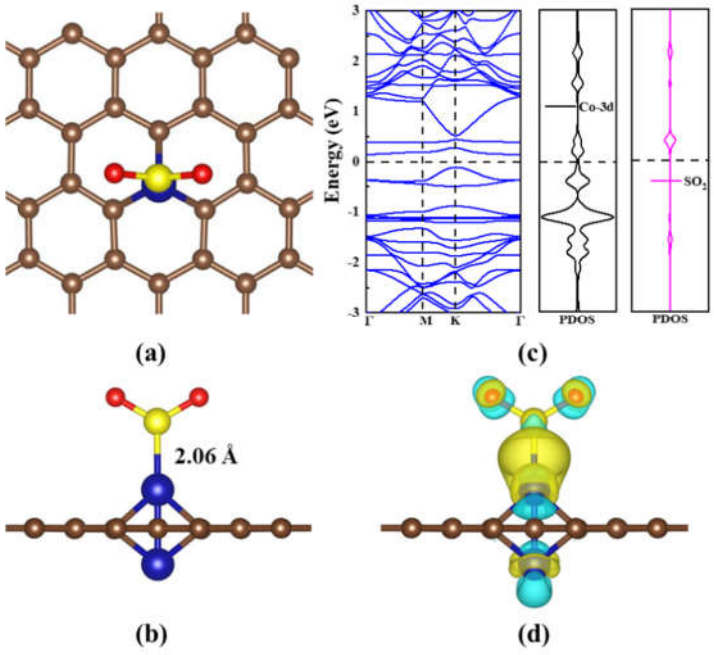

Fig. S17 The most favorable configuration of SO_2 adsorption energy on the Co_2⊥gra structure (top view (a) and side view (b)), energy band structure and PDOS (c), and CDD diagram (d). The isosurface value was set 0.003 e/Å^{-3}.

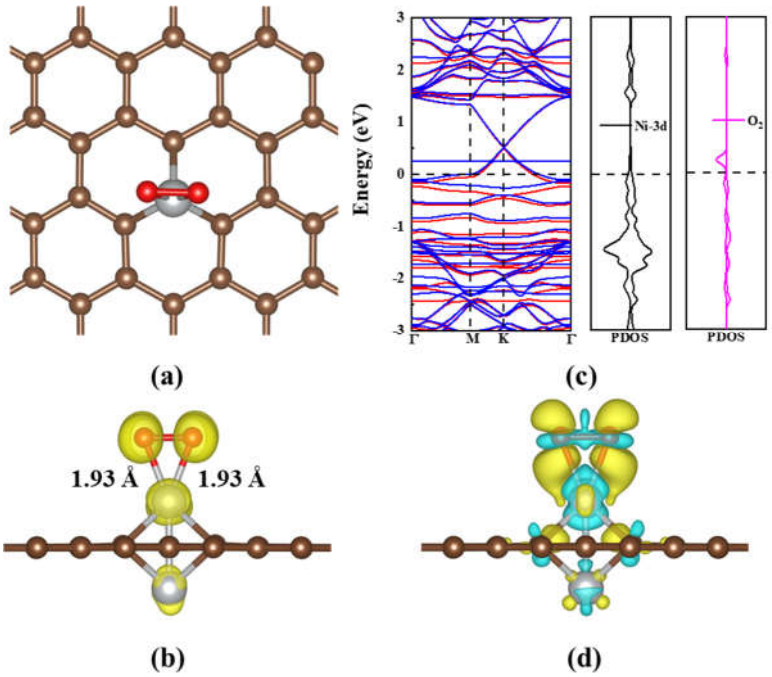

Fig. S18 The most favorable configuration of O_2 adsorption energy on the Ni_2⊥gra structure (top view (a)), spatial spin density distributions (b), energy band structure and PDOS (c), and CDD diagram (d). The isosurface value was set 0.005 e/Å^{-3} for spatial spin density distributions and 0.003 e/Å^{-3} for CDD, respectively.

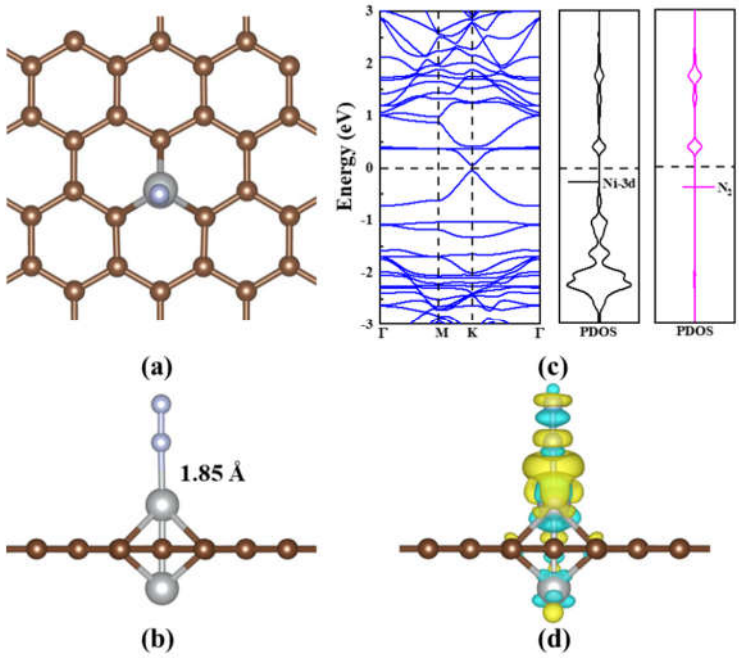

Fig. S19 The most favorable configuration of N_2 adsorption energy on the Ni_2⊥gra structure (top view (a) and side view (b)), energy band structure and PDOS (c), and CDD diagram (d). The isosurface value was set 0.003 e/Å^{-3}.

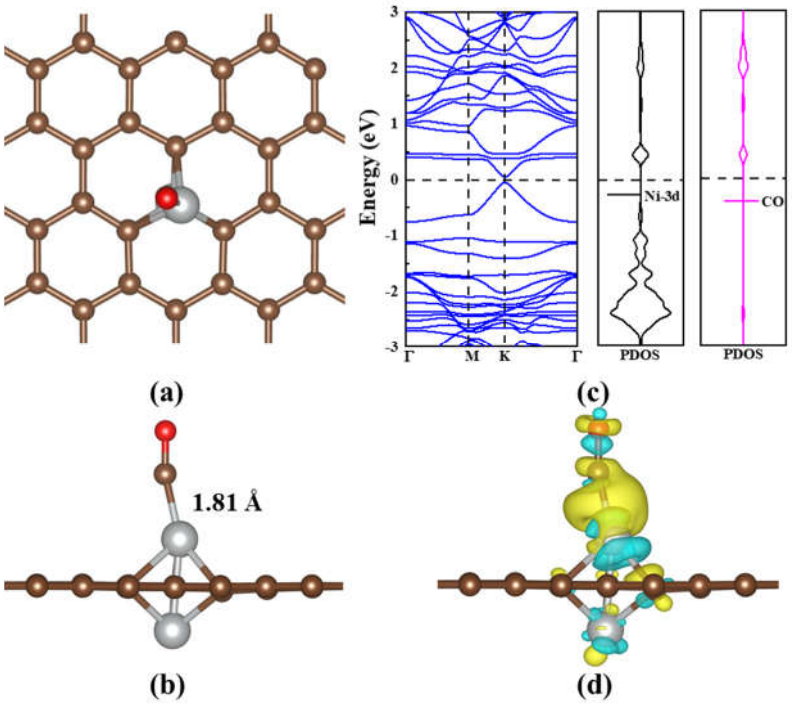

Fig. S20 The most favorable configuration of CO adsorption energy on the Ni_2⊥gra structure (top view (a) and side view (b)), energy band structure and PDOS (c), and CDD diagram (d). The isosurface value was set 0.003 e/Å^{-3}.

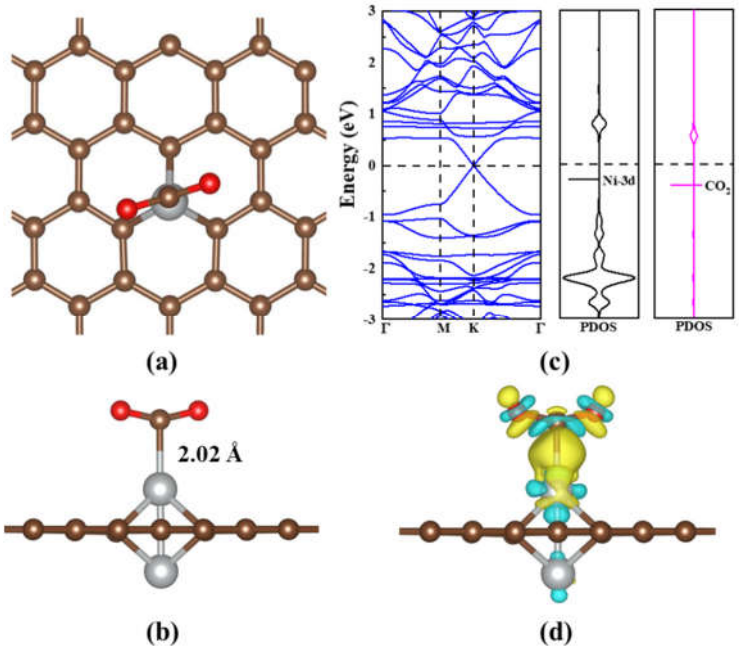

Fig. S21 The most favorable configuration of CO_2 adsorption energy on the Ni_2⊥gra structure (top view (a) and side view (b)), energy band structure and PDOS (c), and CDD diagram (d). The isosurface value was set 0.003 e/Å^{-3}.

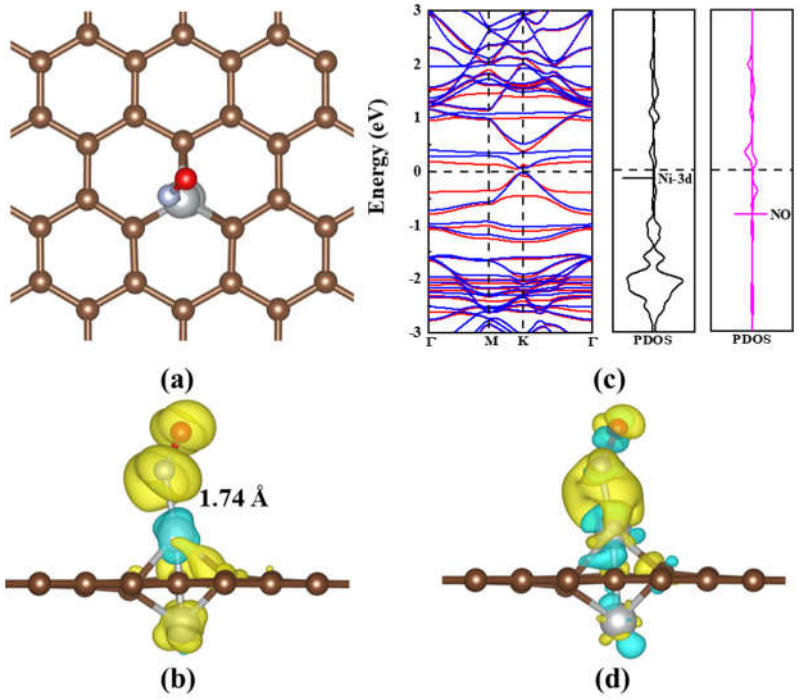

Fig. S22 The most favorable configuration of NO adsorption energy on the Ni_2⊥gra structure (top view (a)), spatial spin density distributions (b), energy band structure and PDOS (c), and CDD diagram (d). The isosurface value was set 0.003 e/Å^{-3}.

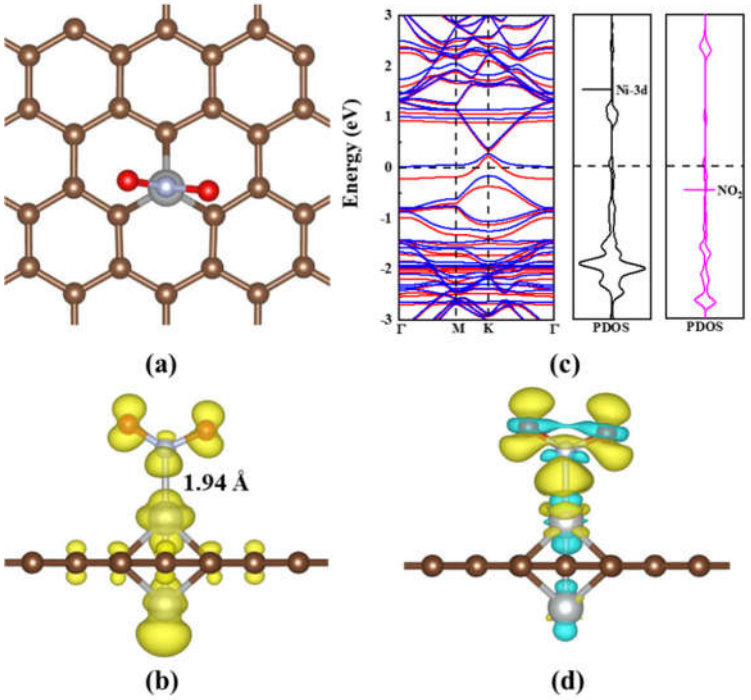

Fig. S23 The most favorable configuration of NO_2 adsorption energy on the Ni_2⊥gra structure (top view (a)), spatial spin density distributions (b), energy band structure and PDOS (c), and CDD diagram (d). The isosurface value was set 0.003 e/Å^{-3}.

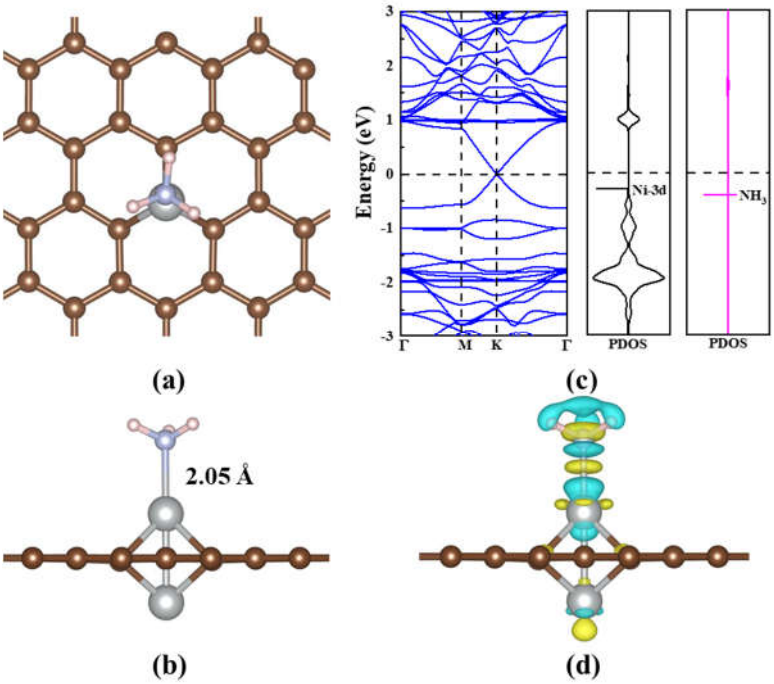

Fig. S24 The most favorable configuration of NH_3 adsorption energy on the Ni_2⊥gra structure (top view (a) and side view (b)), energy band structure and PDOS (c), and CDD diagram (d). The isosurface value was set 0.003 e/Å^{-3}.

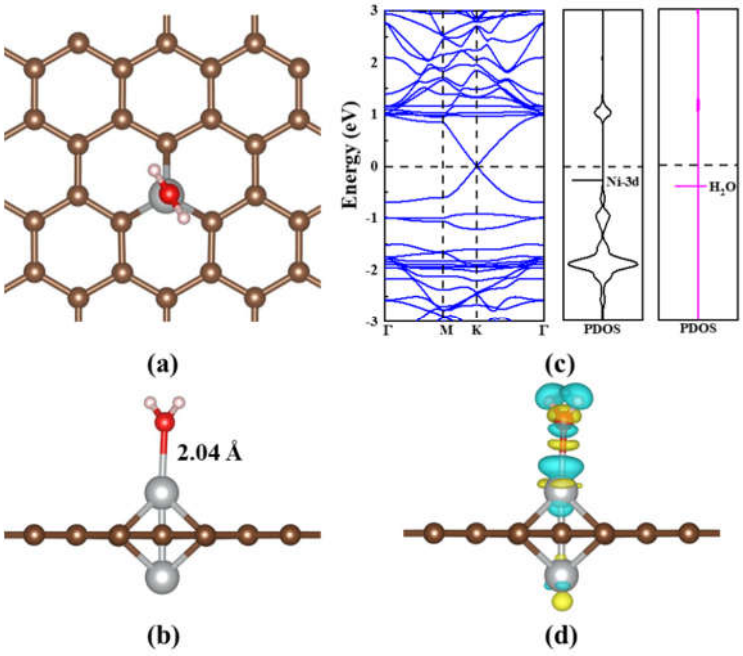

Fig. S25 The most favorable configuration of H_2O adsorption energy on the Ni_2⊥gra structure (top view (a) and side view (b)), energy band structure and PDOS (c), and CDD diagram (d). The isosurface value was set 0.003 e/Å^{-3}.

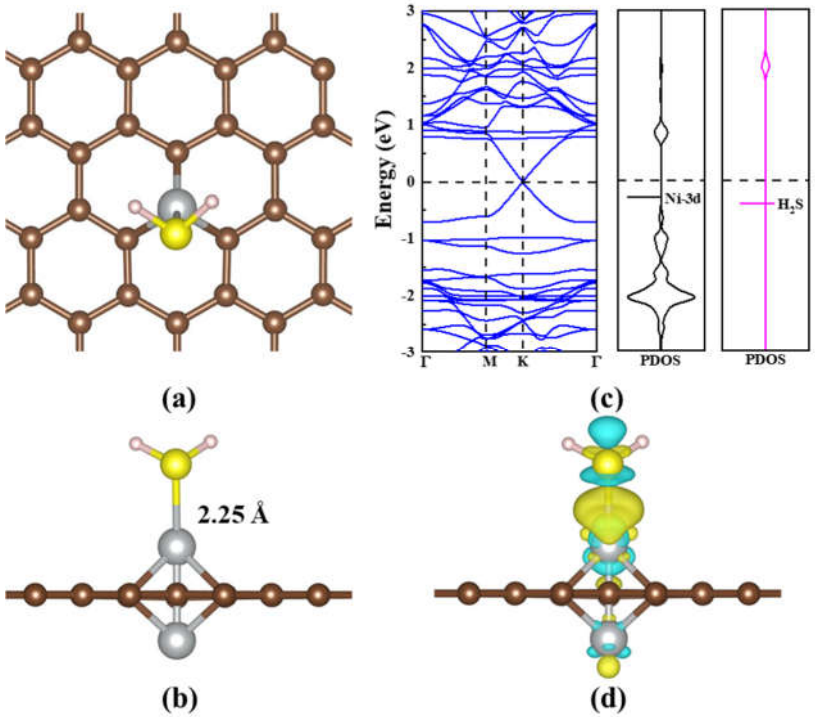

Fig. S26 The most favorable configuration of H_2S adsorption energy on the Ni_2⊥gra structure (top view (a) and side view (b)), energy band structure and PDOS (c), and CDD diagram (d). The isosurface value was set 0.003 e/Å^{-3}.

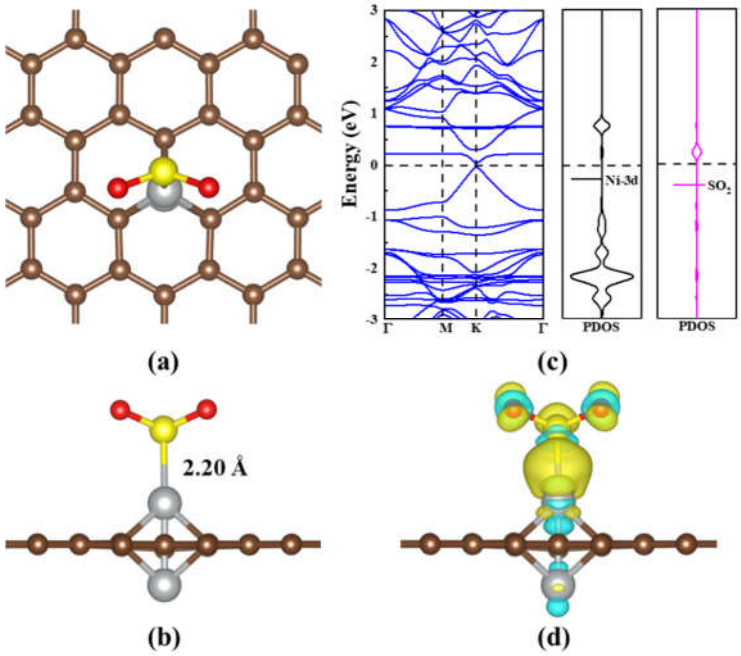

Fig. S27 The most favorable configuration of SO_2 adsorption energy on the Ni_2⊥gra structure (top view (a) and side view (b)), energy band structure and PDOS (c), and CDD diagram (d). The isosurface value was set 0.003 e/Å^{-3}.

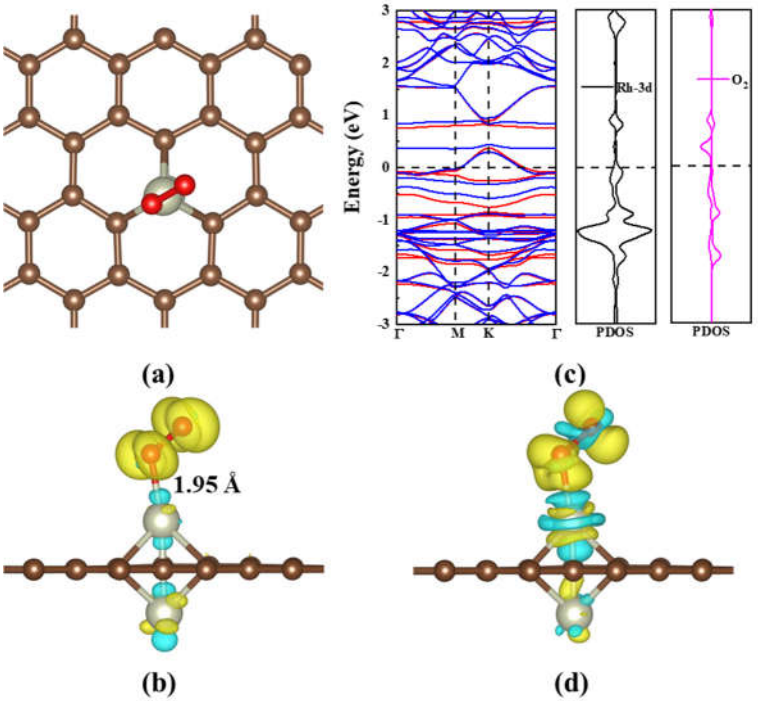

Fig. S28 The most favorable configuration of O_2 adsorption energy on the Rh_2⊥gra structure (top view (a)), spatial spin density distributions (b), energy band structure and PDOS (c), and CDD diagram (d). The isosurface value was set 0.003 e/Å^{-3}.

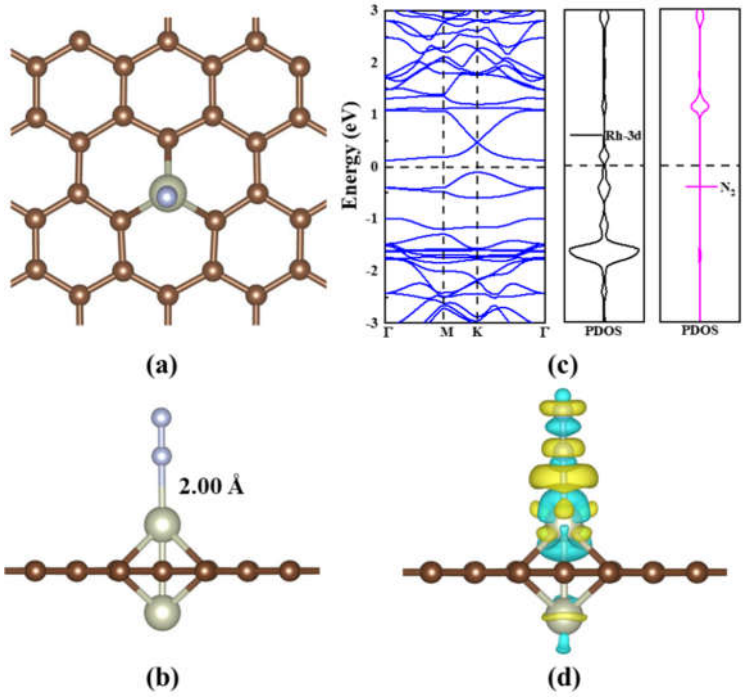

Fig. S29 The most favorable configuration of N_2 adsorption energy on the Rh_2⊥gra structure (top view (a) and side view (b)), energy band structure and PDOS (c), and CDD diagram (d). The isosurface value was set 0.003 e/Å^{-3}.

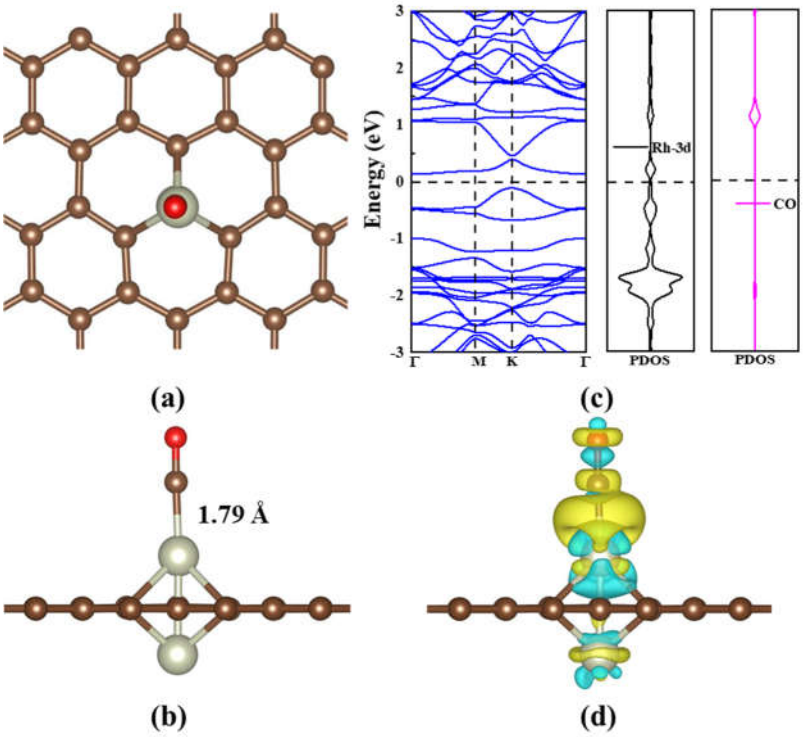

Fig. S30 The most favorable configuration of CO adsorption energy on the Rh_2⊥gra structure (top view (a) and side view (b)), energy band structure and PDOS (c), and CDD diagram (d). The isosurface value was set 0.003 e/Å^{-3}.

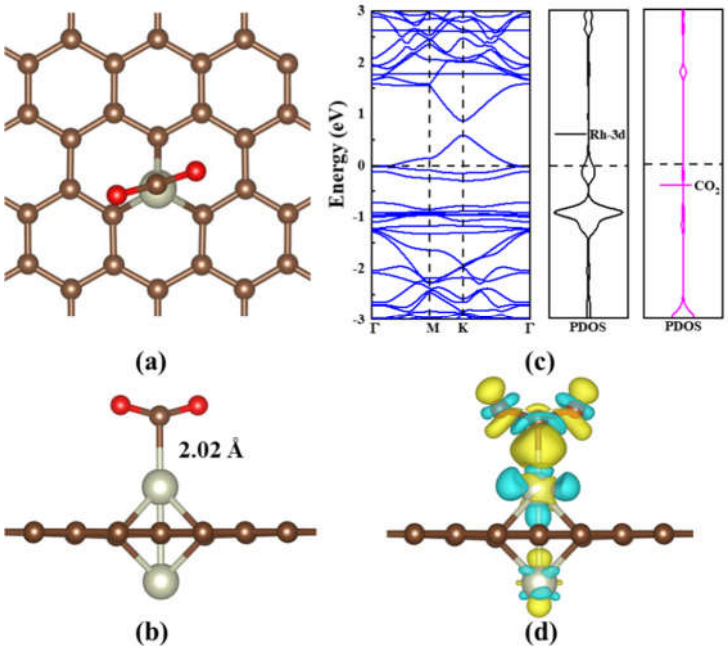

Fig. S31 The most favorable configuration of CO_2 adsorption energy on the Rh_2⊥gra structure (top view (a) and side view (b)), energy band structure and PDOS (c), and CDD diagram (d). The isosurface value was set 0.003 e/Å^{-3}.

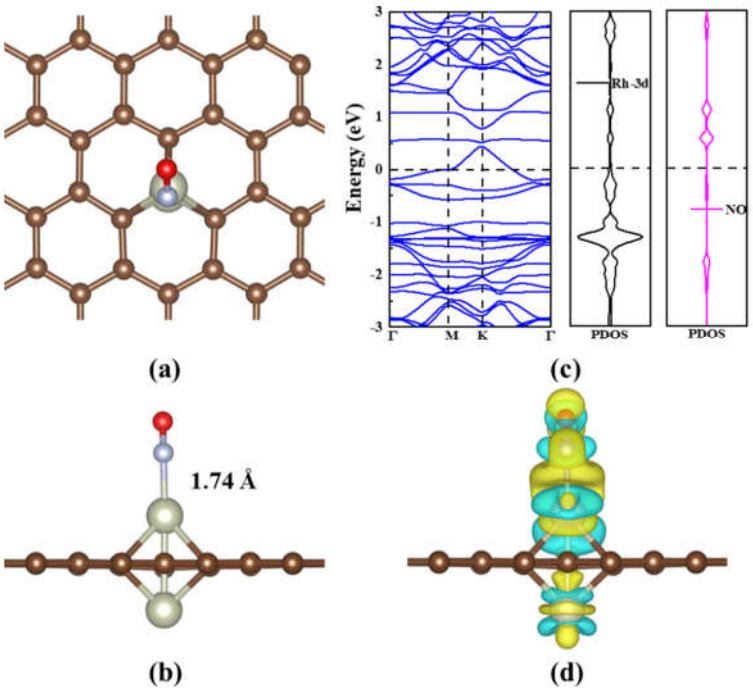

Fig. S32 The most favorable configuration of NO adsorption energy on the Rh_2⊥gra structure (top view (a) and side view (b)), energy band structure and PDOS (c), and CDD diagram (d). The isosurface value was set 0.003 e/Å^{-3}.

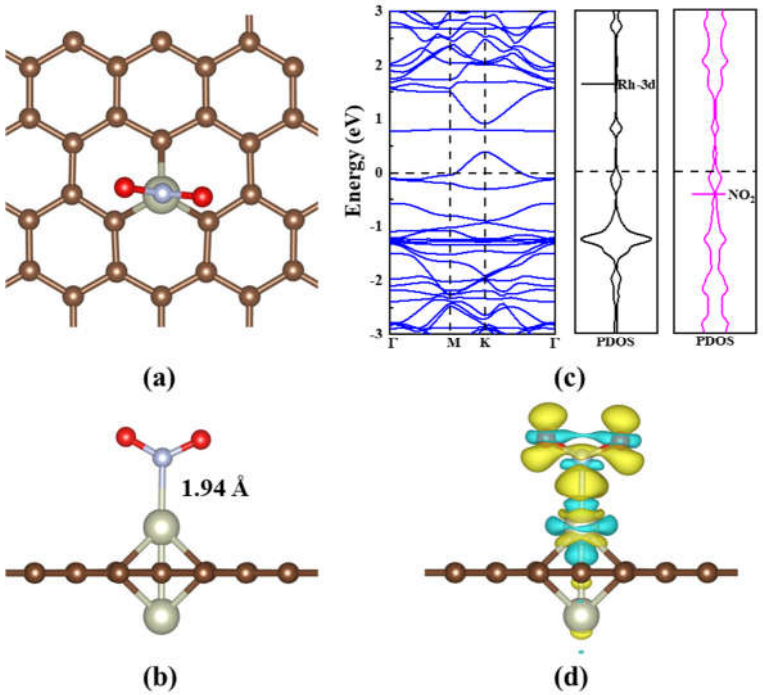

Fig. S33 The most favorable configuration of NO_2 adsorption energy on the Rh_2⊥gra structure (top view (a) and side view (b)), energy band structure and PDOS (c), and CDD diagram (d). The isosurface value was set 0.003 e/Å^{-3}.

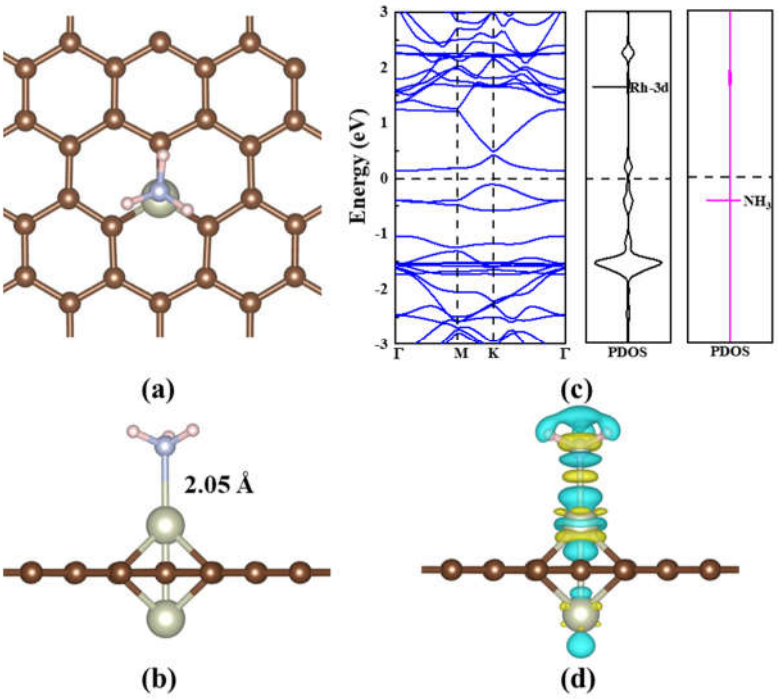

Fig. S34 The most favorable configuration of NH_3 adsorption energy on the Rh_2⊥gra structure (top view (a) and side view (b)), energy band structure and PDOS (c), and CDD diagram (d). The isosurface value was set 0.003 e/Å^{-3}.

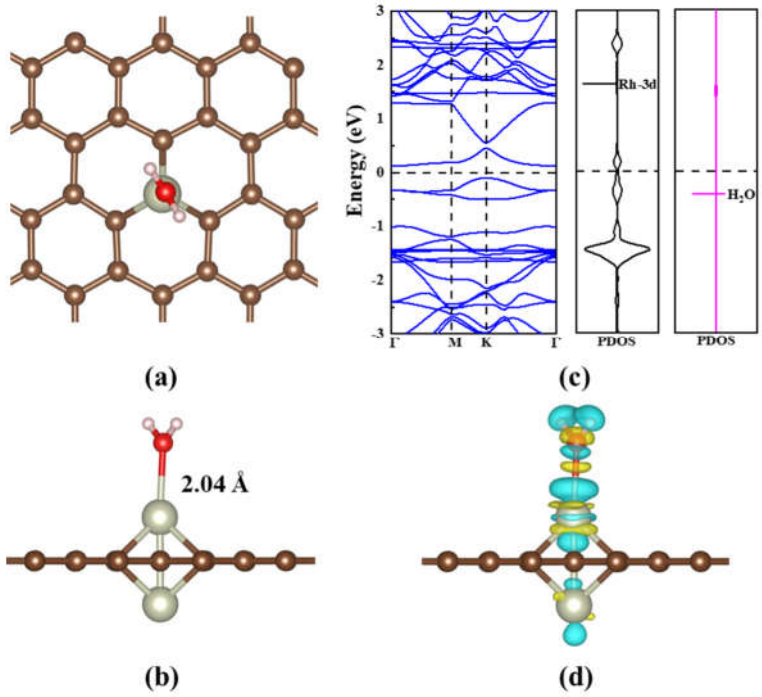

Fig. S35 The most favorable configuration of H_2O adsorption energy on the Rh_2⊥gra structure (top view (a) and side view (b)), energy band structure and PDOS (c), and CDD diagram (d). The isosurface value was set 0.003 e/Å^{-3}.

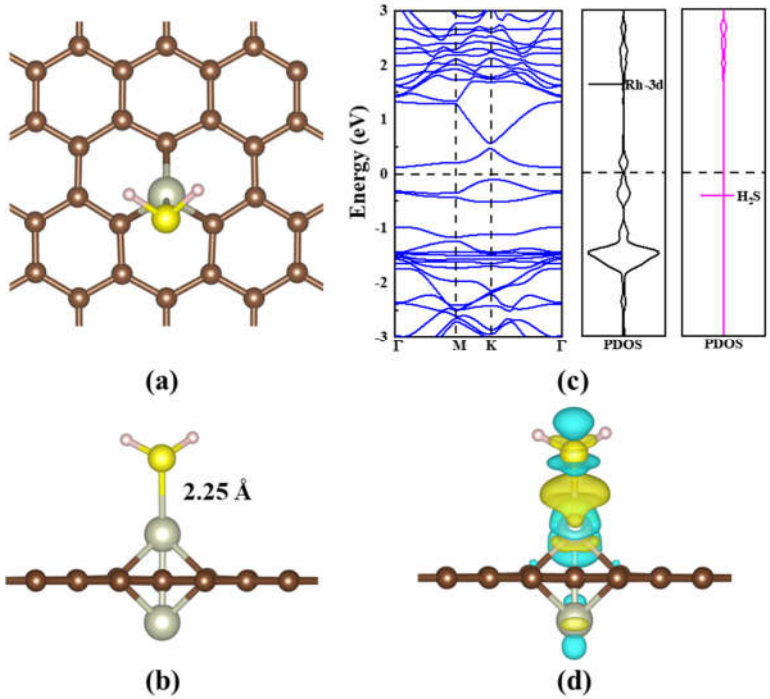

Fig. S36 The most favorable configuration of H_2S adsorption energy on the Rh_2⊥gra structure (top view (a) and side view (b)), energy band structure and PDOS (c), and CDD diagram (d). The isosurface value was set 0.003 e/Å^{-3}.

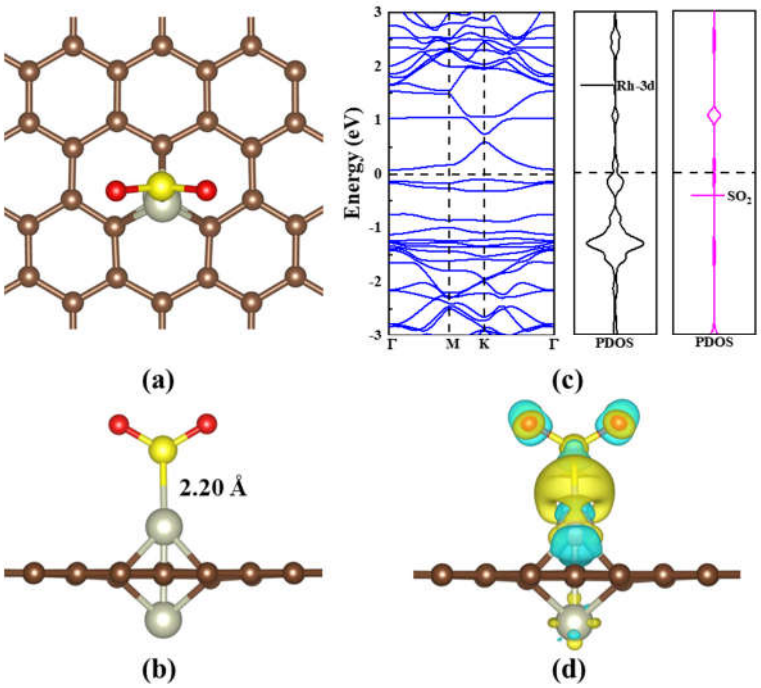

Fig. S37 The most favorable configuration of SO_2 adsorption energy on the Rh_2⊥gra structure (top view (a) and side view (b)), energy band structure and PDOS (c), and CDD diagram (d). The isosurface value was set 0.003 e/Å^{-3}.

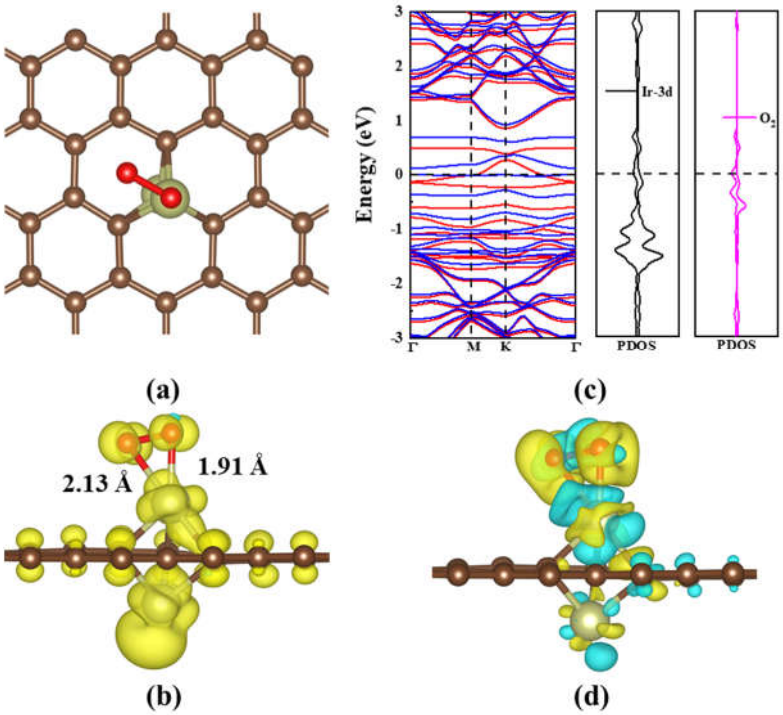

Fig. S38 The most favorable configuration of O_2 adsorption energy on the Ir_2⊥gra structure (top view (a)), spatial spin density distributions (b), energy band structure and PDOS (c), and CDD diagram (d). The isosurface value was set 0.003 e/Å^{-3}.

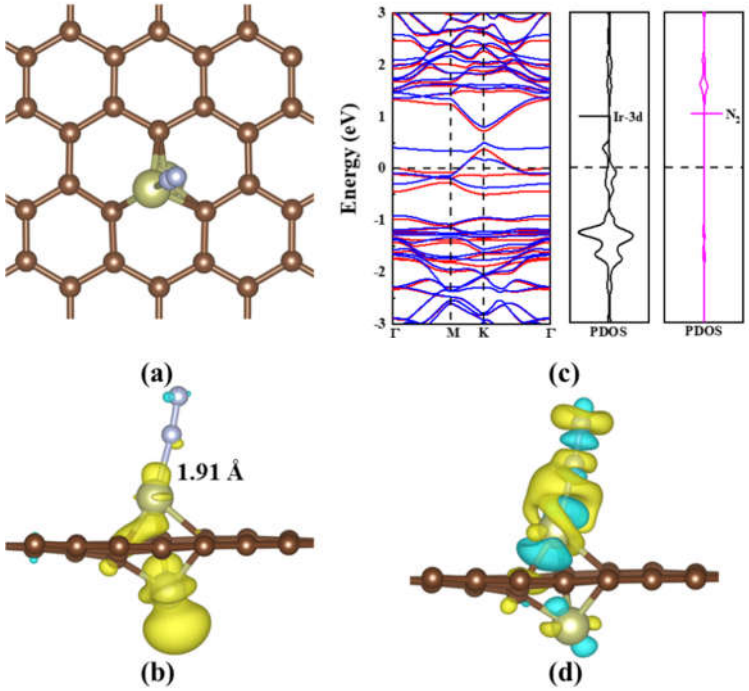

Fig. S39 The most favorable configuration of N_2 adsorption energy on the Ir_2⊥gra structure (top view (a)), spatial spin density distributions (b), energy band structure and PDOS (c), and CDD diagram (d). The isosurface value was set 0.003 e/Å^{-3}.

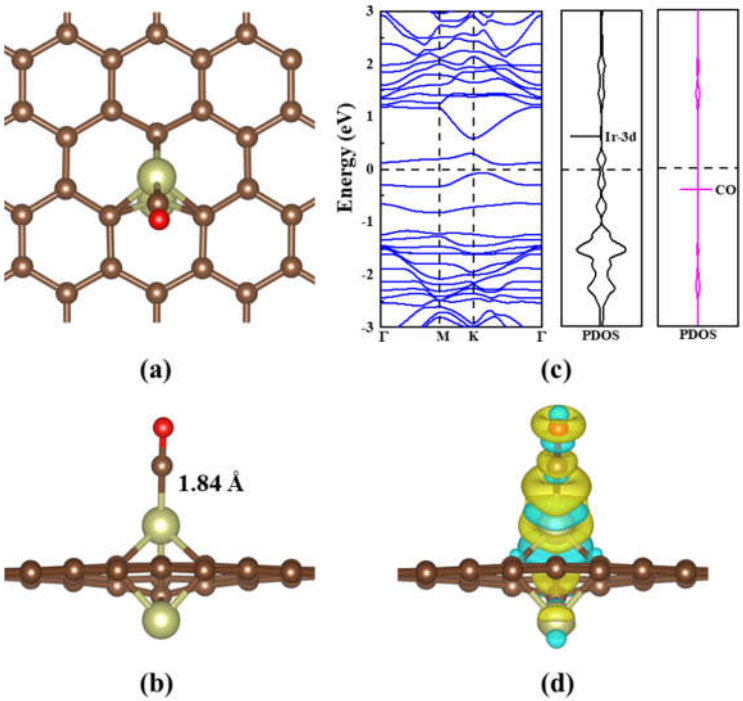

Fig. S40 The most favorable configuration of CO adsorption energy on the Ir_2⊥gra structure (top view (a) and side view (b)), energy band structure and PDOS (c), and CDD diagram (d). The isosurface value was set 0.003 e/Å^{-3}.

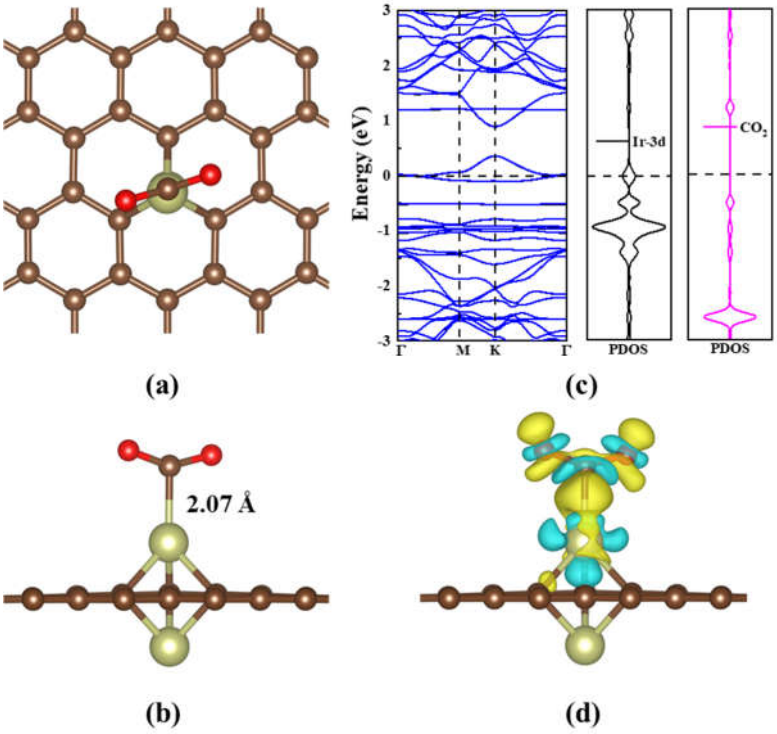

Fig. S41 The most favorable configuration of CO_2 adsorption energy on the Ir_2⊥gra structure (top view (a) and side view (b)), energy band structure and PDOS (c), and CDD diagram (d). The isosurface value was set 0.003 e/Å^{-3}.

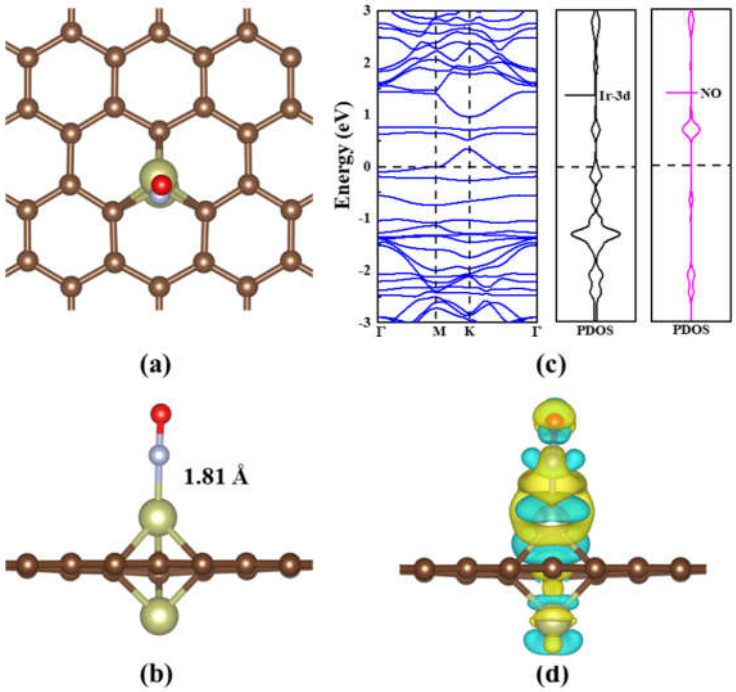

Fig. S42 The most favorable configuration of NO adsorption energy on the Ir_2⊥gra structure (top view (a) and side view (b)), energy band structure and PDOS (c), and CDD diagram (d). The isosurface value was set 0.003 e/Å^{-3}.

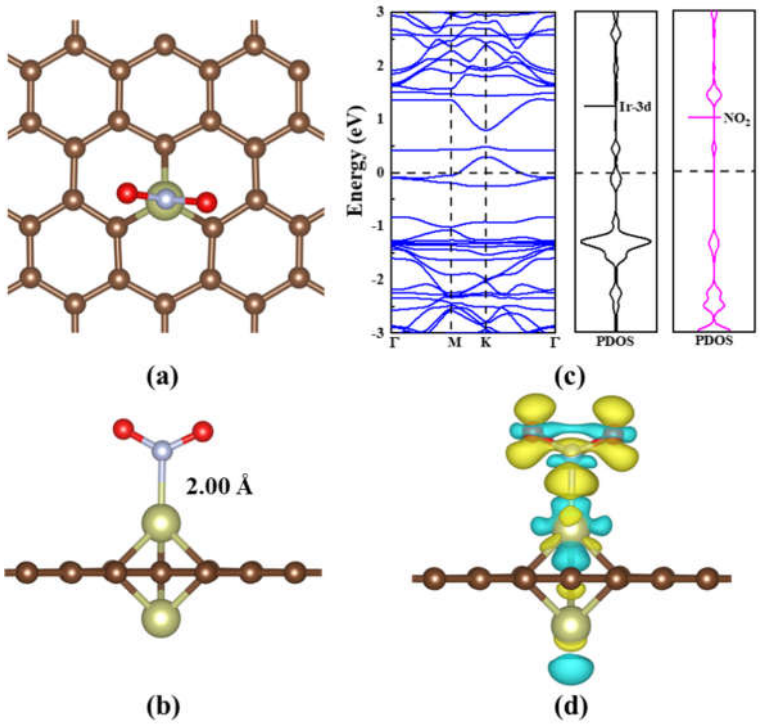

Fig. S43 The most favorable configuration of NO_2 adsorption energy on the Ir_2⊥gra structure (top view (a) and side view (b)), energy band structure and PDOS (c), and CDD diagram (d). The isosurface value was set 0.003 e/Å^{-3}.

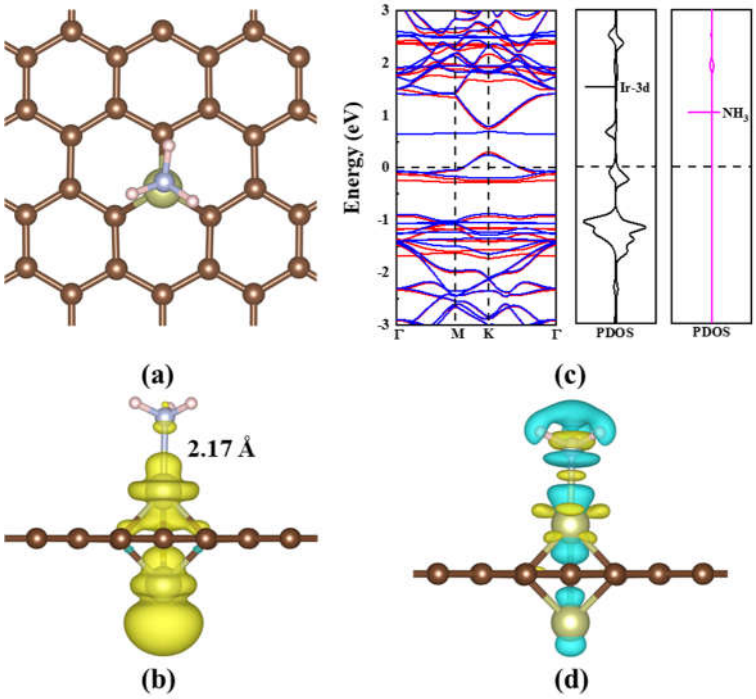

Fig. S44 The most favorable configuration of NH_3 adsorption energy on the Ir_2⊥gra structure (top view (a)), spatial spin density distributions (b), energy band structure and PDOS (c), and CDD diagram (d). The isosurface value was set 0.003 e/Å^{-3}.

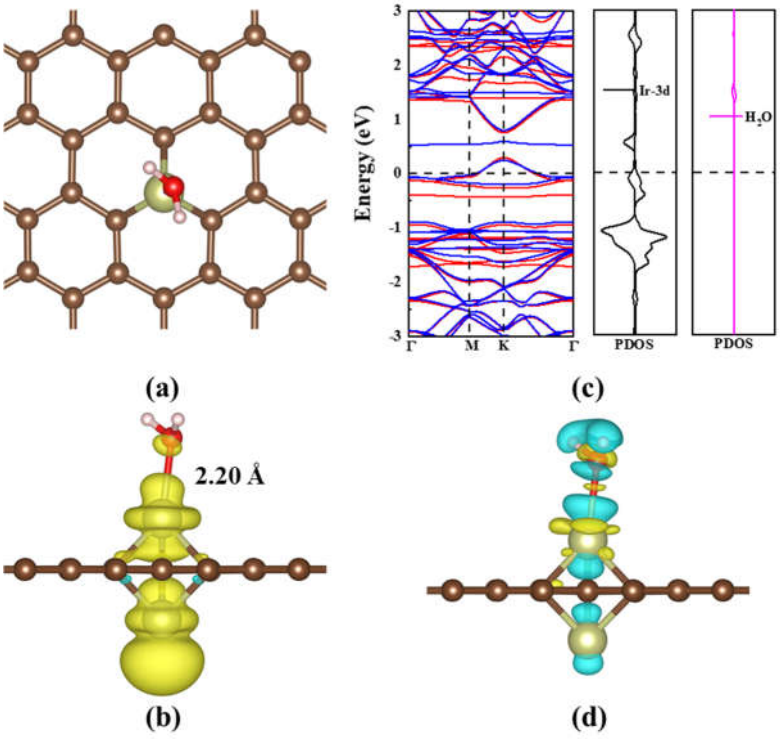

Fig. S45 The most favorable configuration of H_2O adsorption energy on the Ir_2⊥gra structure (top view (a)), spatial spin density distributions (b), energy band structure and PDOS (c), and CDD diagram (d). The isosurface value was set 0.003 e/Å^{-3}.

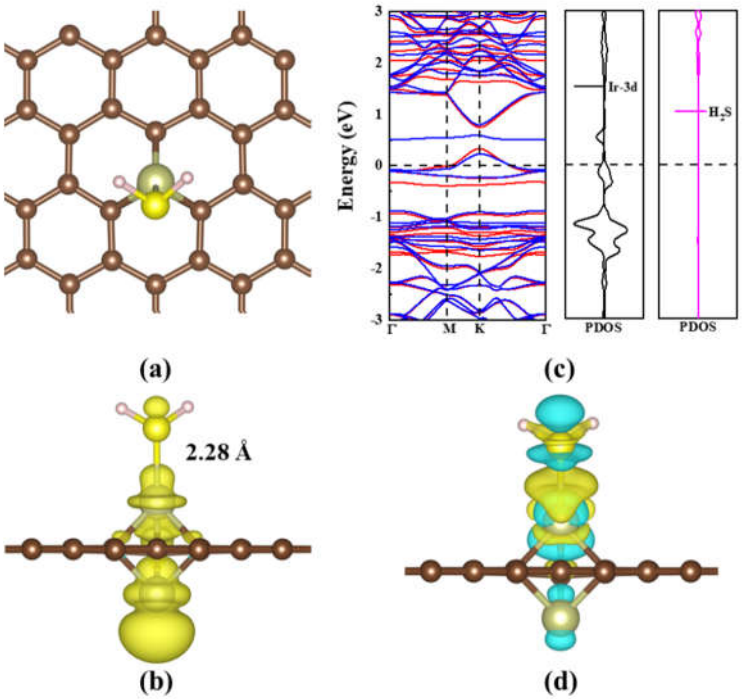

Fig. S46 The most favorable configuration of H_2S adsorption energy on the Ir_2⊥gra structure (top view (a)), spatial spin density distributions (b), energy band structure and PDOS (c), and CDD diagram (d). The isosurface value was set 0.003 e/Å^{-3}.

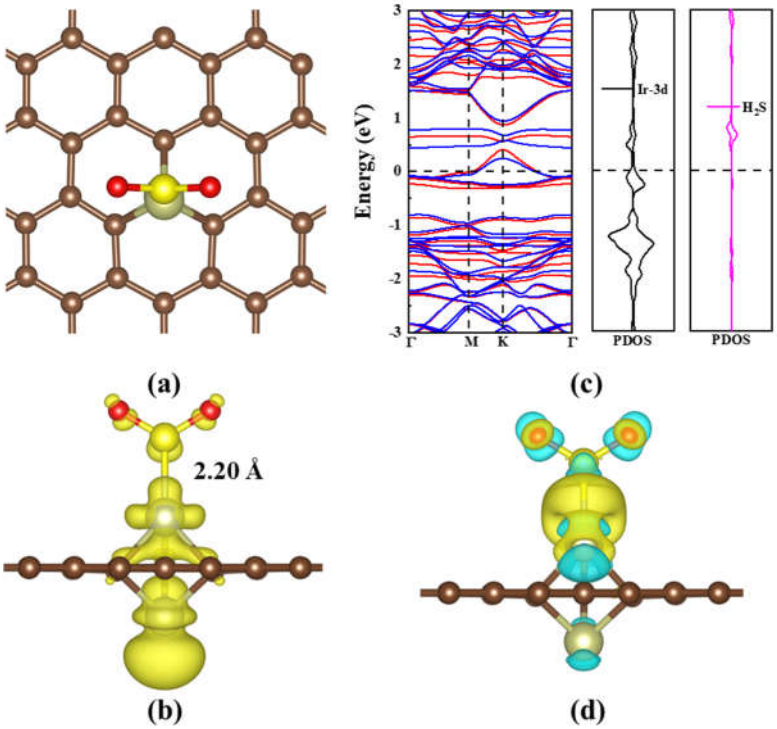

Fig. S47 The most favorable configuration of SO_2 adsorption energy on the Ir_2⊥gra structure (top view (a)), spatial spin density distributions (b), energy band structure and PDOS (c), and CDD diagram (d). The isosurface value was set 0.003 e/Å^{-3}.

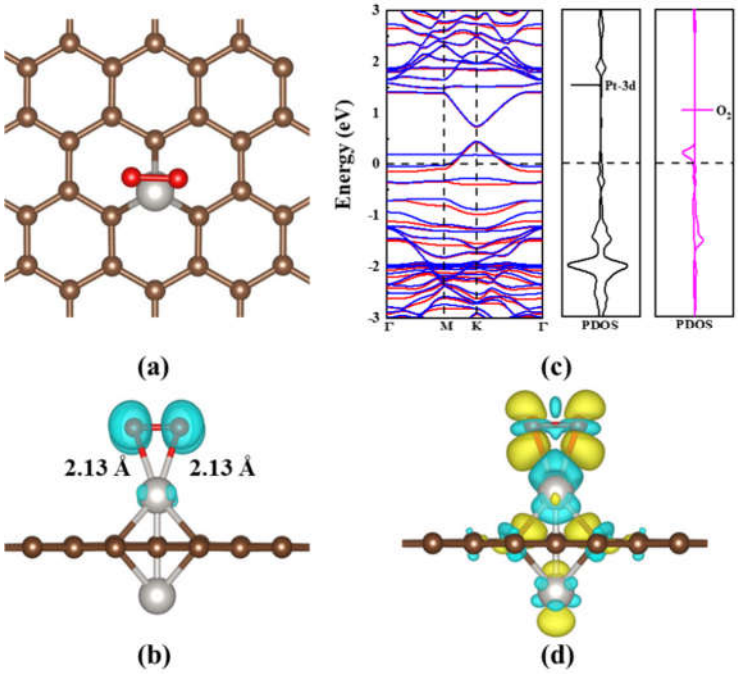

Fig. S48 The most favorable configuration of O_2 adsorption energy on the Pt_2⊥gra structure (top view (a)), spatial spin density distributions (b), energy band structure and PDOS (c), and CDD diagram (d). The isosurface value was set 0.003 e/Å^{-3}.

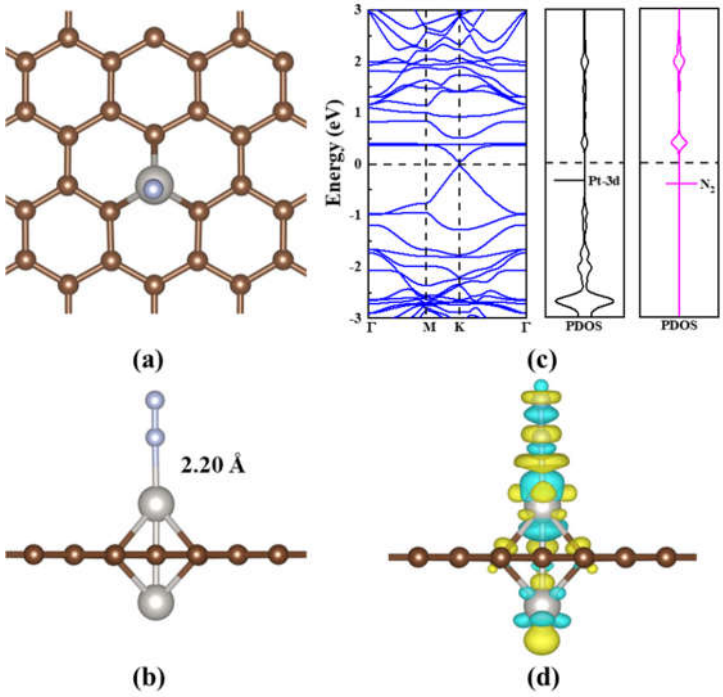

Fig. S49 The most favorable configuration of N_2 adsorption energy on the Pt_2⊥gra structure (top view (a) and side view (b)), energy band structure and PDOS (c), and CDD diagram (d). The isosurface value was set 0.003 e/Å^{-3}.

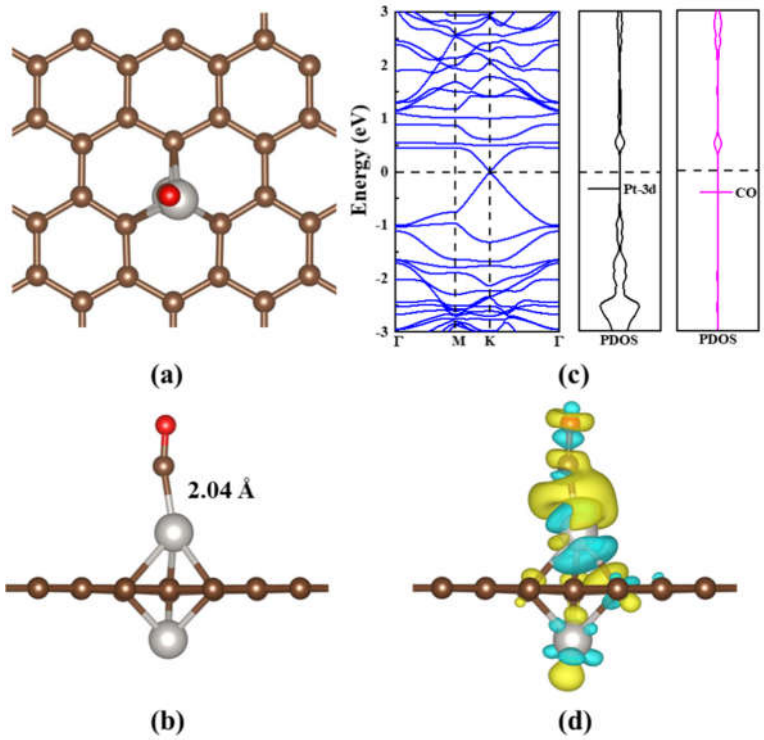

Fig. S50 The most favorable configuration of CO adsorption energy on the Pt_2⊥gra structure (top view (a) and side view (b)), energy band structure and PDOS (c), and CDD diagram (d). The isosurface value was set 0.003 e/Å^{-3}.

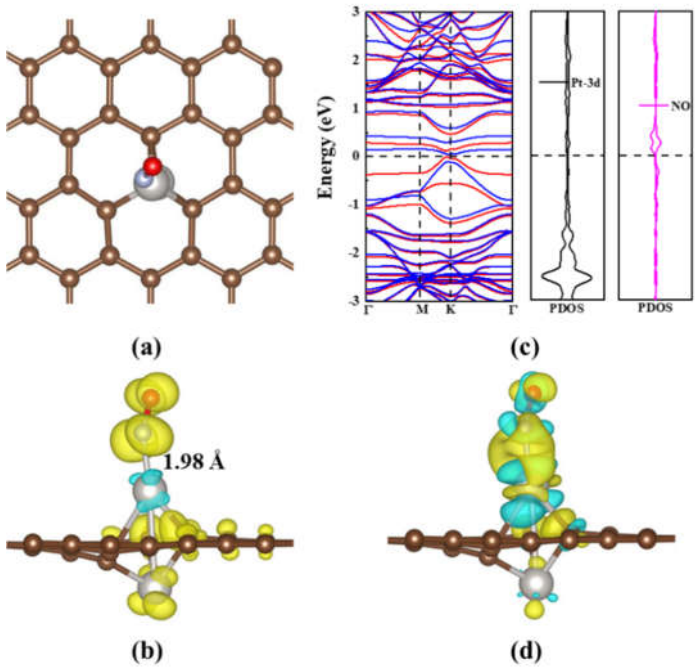

Fig. S51 The most favorable configuration of NO adsorption energy on the Pt_2⊥gra structure (top view (a)), spatial spin density distributions (b), energy band structure and PDOS (c), CDD diagram (d). The isosurface value was set 0.003 e/Å^{-3}.

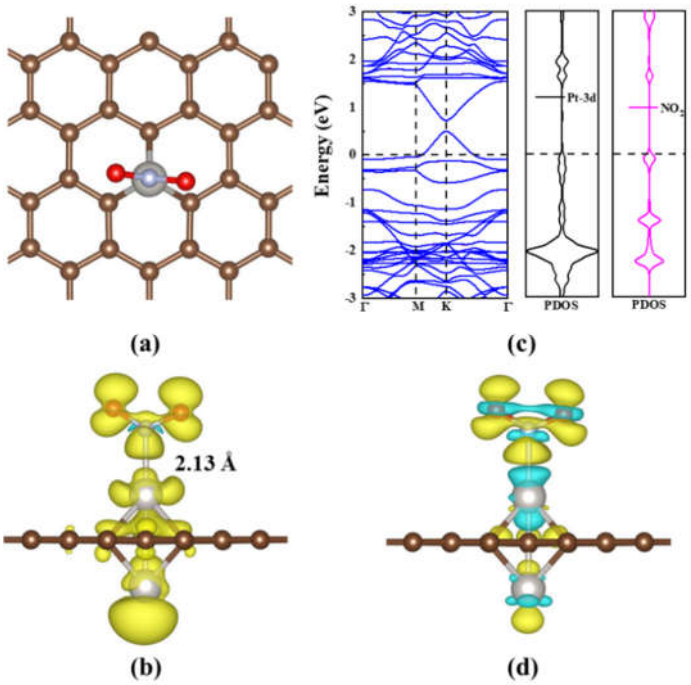

Fig. S52 The most favorable configuration of NO_2 adsorption energy on the $Pt_2 \perp$ gra structure (top view (a)), spatial spin density distributions (b), energy band structure and PDOS (c), and CDD diagram (d). The isosurface value was set 0.0003 e/Å^{-3} for spatial spin density distributions and 0.003 e/Å^{-3} for CDD, respectively.

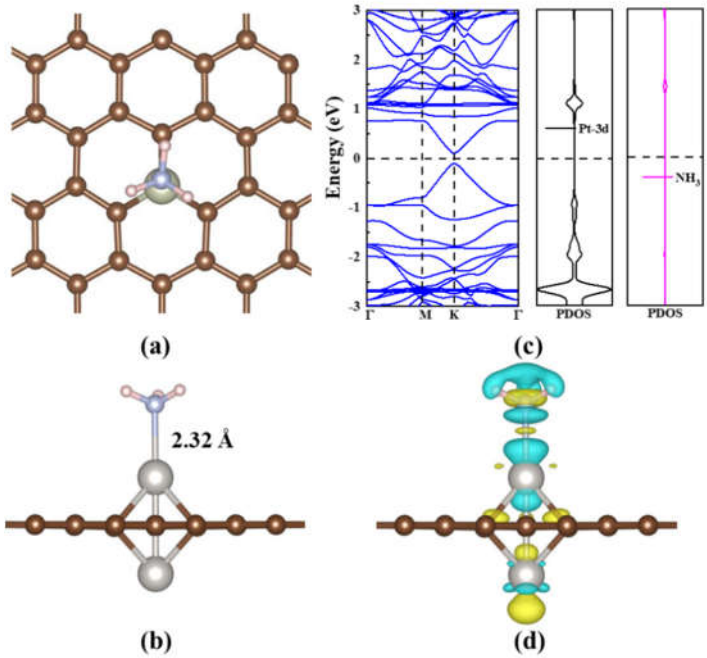

Fig. S53 The most favorable configuration of NH_3 adsorption energy on the $Pt_2 \perp$ gra structure (top view (a) and side view (b)), energy band structure and PDOS (c), and CDD diagram (d). The isosurface value was set 0.003 e/Å^{-3}.

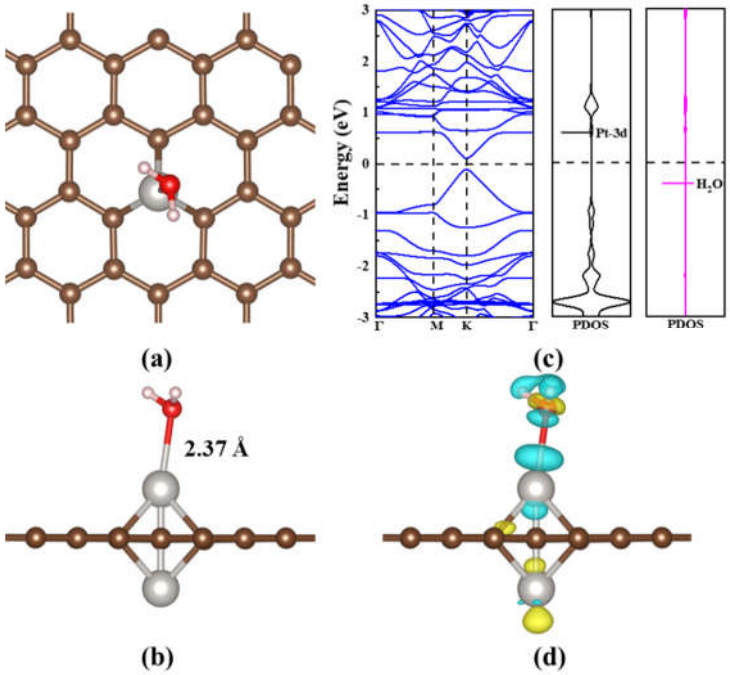

Fig. S54 The most favorable configuration of H_2O adsorption energy on the Pt_2⊥gra structure (top view (a) and side view (b)), energy band structure and PDOS (c), and CDD diagram (d). The isosurface value was set 0.003 e/Å^{-3}.

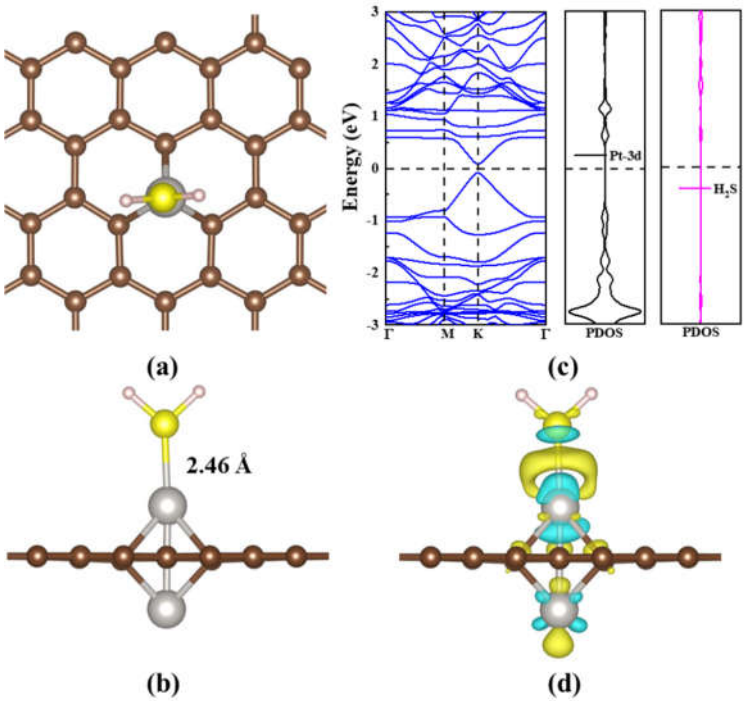

Fig. S55 The most favorable configuration of H_2S adsorption energy on the Pt_2⊥gra structure (top view (a) and side view (b)), energy band structure and PDOS (c), and CDD diagram (d). The isosurface value was set 0.003 e/Å^{-3}.

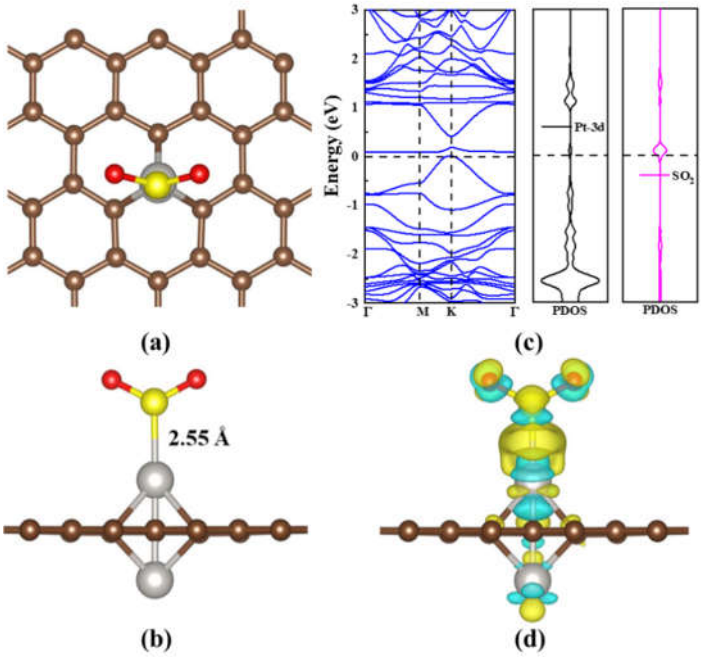

Fig. S56 The most favorable configuration of SO_2 adsorption energy on the Pt_2⊥gra structure (top view (a) and side view (b)), energy band structure and PDOS (c), and CDD diagram (d). The isosurface value was set 0.003 e/Å^{-3}.

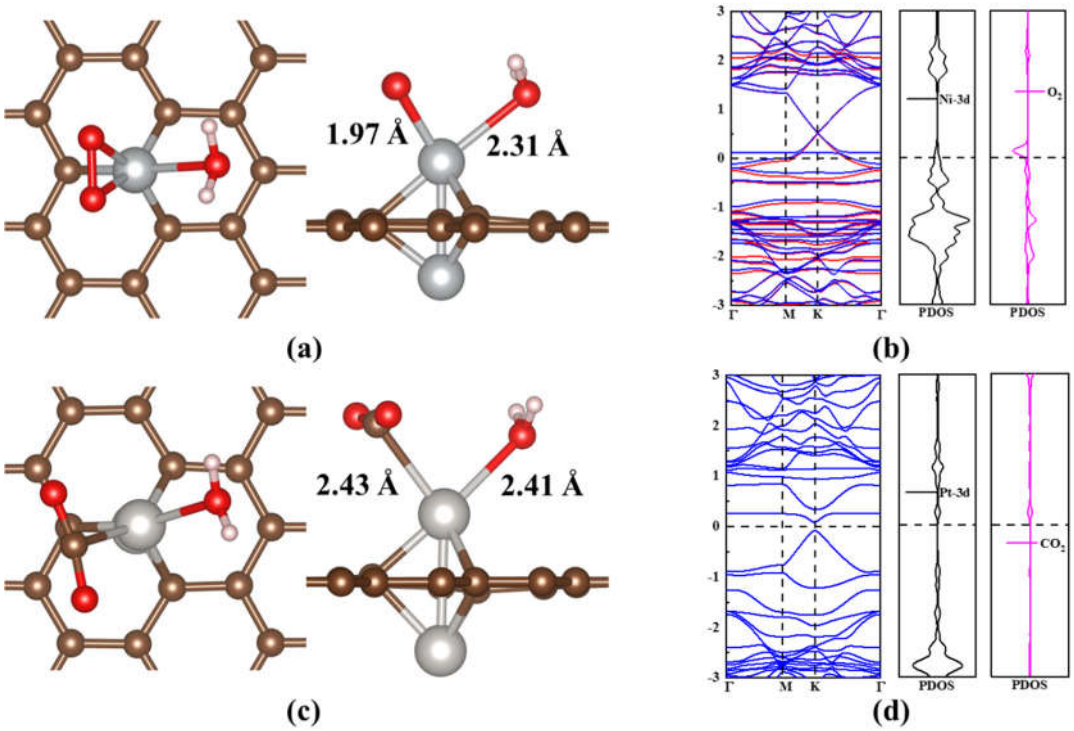

Fig. S57 The most favorable configuration of O_2/CO_2 and H_2O co-adsorption on the Ni_2⊥gra/Pt_2⊥gra structure (a/c), and their corresponding energy band structure and PDOS (b/d).